A UNIFIED THEORY FOR UPSCALING FRACTURED, VUGGY RESERVOIR MODELS – THE DEVELOPMENT OF NOVEL TRANSFER FUNCTIONS

A Thesis

by

SUNHUA GAO

Submitted to the Office of Graduate and Professional Studies of
Texas A&M University
in partial fulfillment of the requirements for the degree of

MASTER OF SCIENCE

Chair of Committee,	John E. Killough
Committee Members,	Eduardo Gildin
	Maria A. Barrufet
Head of Department,	A. Daniel Hill

August 2016

Major Subject: Petroleum Engineering

ABSTRACT

More than half of the world's oil and gas reserves are found in carbonate reservoirs. Most carbonates are fractured, vuggy reservoirs which can be defined as reservoirs that contain matrix, fractures and vugs. Vugs in such reservoirs can be isolated or connected to a global fracture system. Numerical modeling of naturally fractured, vuggy reservoirs presents many challenges due to the coexistence of three very different media and their complex interaction on multiple scales. With current computing capabilities, conventional fine-scale, single porosity models are not practical for modeling such reservoirs on the multi-well or the field-wide scale due to the massive number of grid blocks. Thus, an effective approach would be through a triple continuum model where matrix, fractures and vugs are separated into three different porosity systems. This work investigates mass exchange between different media with the final objective of providing a unified theory for the use of transfer functions in upscaling fractured, vuggy reservoir simulation models.

In a triple continuum model, the fracture system provides the path for global fluid flow, while vuggy and matrix continua mostly contribute to the fluid storage; thus, the interporosity fluid exchange becomes very important and dominates the oil displacement of such reservoirs. Through the use of fine-grid explicit simulation models, this research analyzed the complex mechanisms of mass transfers between each two porosity systems. Different concept models are generated to show the effect of vug fraction, shape and distribution on oil displacement. New transfer functions for the

simulation of 3D two phase fluid flow in the triple continuum model to capture the complex flow mechanisms and emulate the results of the fine-scale, single porosity model are also provided. In addition, a general procedure of incorporating the proposed transfer functions into the triple continuum model along with a novel upscaling technique is presented.

This paper provides the first investigation of the complex fluid exchange among different media in fractured, vuggy reservoirs. Results show that the use of the proposed transfer functions helps to reduce the size of simulation models for fractured, vuggy reservoirs, and improve the computation speed by orders of magnitude, while providing an accurate representation of the fine-scale results.

DEDICATION

To Lie,

Because of you, I know I'll always be blessed with love.

ACKNOWLEDGEMENTS

I would like to thank my committee chair, Dr. John E. Killough for his invaluable guidance, inspiration and support concerning my research. This work would not have been possible without his instruction. Being his student is one of the best things that happened in my life.

I would like to thank Dr. Eduardo Gildin and Dr. Maria A. Barrufet for serving on my advisory committee and giving me valuable suggestions for my thesis. I also wish to thank the rest of the Petroleum Engineering Department faculty for their contributions to my academic achievement. I would like to extend a big thanks to Jie He, Mohamed Fadlelmula, Xuyang Guo and other group members for all their help with my research; to Hewei Tang who cared about me and encouraged me to finish my thesis as soon as possible.

I would like to thank Qatar Foundation for the financial support to this research work.

My great gratitude extends to Dr. Yuetian Liu, Dr. Shicheng Zhang and Dr. Baojiang Sun from China University of Petroleum for their support of my overseas study.

Finally, thanks to my parents for their endless love and support.

NOMENCLATURE

B	Formation volume factor, RB/STB
C	Total compressibility, 1/Psia
D	Depth, ft
F_v	Vug fraction
g	Gravitational acceleration, m^2/s
H_{vug}	Vug length along the direction of pressure gradient, ft
k	Absolute permeability, md
k_r	Relative permeability
l	Characteristic length of heterogeneous region, ft
L_x	length of grid block, ft
N_f	Number of fractures connected to the vug
n	Number of normal sets of fractures
p	Block pressure, psia
p_i	Initial pressure, psia
p_{cap}	Capillary pressure, Psia
q	Mass exchange rate, lbm/day
S	Saturation
T	Tansmissibility, md·ft

t	Time, day
V	Volume, ft^3
σ	Shape factor, $1/ft^2$
ρ	Density, lbm/ft^3
γ	Gravity constant
μ	Viscosity, cp
λ	Mobility, 1/cp
Φ	Potential, psia
ϕ	Porosity

TABLE OF CONTENTS

Page

LIST OF FIGURES

Page

LIST OF TABLES

Page

CHAPTER I

INTRODUCTION

1.1 Problem Definition

Fractured, vuggy reservoirs can be defined as reservoirs that contain long range fractures, matrix, and vugs with various size and distribution. Numerical modeling of naturally fractured, vuggy reservoirs presents many challenges due to the coexistence of three very different media and their complex interaction on multiple scales. The interaction of one medium with another is represented by an interporosity transfer function, an idea that was originally proposed by Barenblatt et al. (1960). The mechanisms of multiphase flow exchange between those three media depend on the combined effects of matrix-block size, connectivity and wettability of three media, rock and fluid characteristics, pressure and saturation history (Chilingar, 1996). Those are the major reasons that make the modeling of interporosity flow behavior very complicated. Since interporosity flow dominates the fluid recovery, it is important that adequate transfer functions are incorporated in any simulation models.

In addition, the multi-scale heterogeneous nature of the vug system and various vug/fracture connected networks will add another challenge to the modeling and simulation of fractured, vuggy reservoirs. The vug geometries, connectivity and spatial distribution have a great impact on the fluid behavior in such reservoirs (Popov et al., 2007). Vuggy pore space can be substituted into two groups: separate vugs that are isolated by matrix rock and connected vugs that are connected to the overall fracture

network (Lucia, 1999, Jennings et al., 2001). The size of separate vugs can vary from millimeters to centimeters in diameter depending upon their origin (Yu-Shu Wu et al., 2006). Connected vugs are hard to characterize because the vugs are often larger than the cross section areas of core samples (Lucia, 2007). Fractures and vugs can form various types of connected networks which highly change the petrophysical characteristics of the formation rock. The performance of the simulation model is significantly impacted by how robustly these features are characterized and modeled.

Another challenge arises from upscaling the fine-grid model into a triple-continuum coarse model in that the coarse model tends to underestimate the oil recovery. This is caused by numerical dispersion, so that the saturation front doesn't exist in the coarse model. Moreover, the fact that the capillary pressure in the coarse model is determined by average water saturation in the matrix grid block will also influence accuracy of the upscaling solution.

With current computing capabilities, conventional fine-scale, single porosity models are not practical for modeling fractured, vuggy reservoirs on the multi-well or the field-wide scale due to the massive number of grid blocks. A triple-continuum reservoir model based on a commercial simulator is presented as an effective approach to modeling fractured, vuggy reservoirs on the coarse scale. This model consists of three different porosity systems, i.e. low permeability matrix, connected fractures and discontinuous vugs that can be isolated or connected to the fracture network. When the global flow occurs through fracture system, and when vuggy and matrix continua mostly contribute to the fluid storage; the interporosity flow dominates the oil displacement of

such reservoirs. Therefore, transfer functions that describe the interporosity flow are the heart of the triple-continuum reservoir model. Although many progress has been made on matrix-fracture transfer function, there hardly has been any investigations on interporosity flow between vugs and the other two media. This paper investigates the mass exchange between three different media with the final objective of providing a unified theory for the use of transfer functions in upscaling fractured, vuggy reservoir simulation models. At this point, we should understand that a triple-continuum model shall not be deemed as rigorous if the above mentioned challenges cannot be solved appropriately.

1.2 Outline

This dissertation is organized as follows:

The second chapter provides a review of the most commonly used transfer functions in dual porosity models. Their formulations and limitations will be discussed in order to gain a comprehensive understanding on the use of transfer functions to describe interporosity flow, and thus to lay a good foundation for the development of matrix-vug transfer function and facture-vug transfer function in this study. In addition, the previous proposed approaches for modeling fluid flow through fractured, vuggy rock will be discussed in order to justify the necessity of using the triple-continuum model for field scale simulation.

The third chapter focuses on the fluid exchange between matrix and vug systems where vugs are isolated by matrix from the overall facture network. Three dimensional

conceptual models based on the actual vuggy formation data is introduced in the first section. The second section starts with the sensitivity analysis of the vug spatial distribution on single-phase fluid exchange, and then through a history matching procedure, achieves the shape factor equations at the end. In the third section, mechanisms of two phase fluid exchange between matrix and vugs are first discussed, and a general process is proposed to generate a dynamic matrix-vug transfer function that can incorporate all the mechanisms. The last section proposes a novel upscaling method by adding a transmissibility multiplier table as an extra connection term of the proposed transfer function in order to improve the accuracy of the triple-continuum, coarse model.

The fourth chapter investigates the fluid exchange between fracture and vug systems. Based on the simulation of fine-scale, explicit models, the mechanisms of two-phase fluid exchange between fracture and vug systems are discussed, and then the effects of vug fraction (vug pore volume per coarse grid block volume) and connectivity on fluid exchange are analyzed. A general process is proposed to generate a two phase fracture-vug transfer function which combines a dynamic shape factor with the pseudo capillary pressure of vug system.

The fifth chapter gives a conclusion of the results obtained through this work along with recommendations for future work in this area.

CHAPTER II

LITERATURE REVIEW

Since the 1960s, the study of fluid flow through naturally fractured reservoirs has been a hot spot in petroleum engineering research area, and many significant progress has been made on dual porosity models. Most commonly used transfer functions in dual porosity models are discussed in this chapter along with their limitations, to provide the foundation for developing two phase flow transfer functions for triple media-matrix, fractures and vugs. This chapter also discusses several studies that has been conducted to modeling naturally fractured, vuggy reservoirs for the last decade.

2.1 Transfer Functions

The interaction of one porosity system with another is represented by an interporosity transfer function. This idea was proposed originally by Barenblatt et al. (1960), and later become the base of other developed matrix-facture transfer functions (Abushaikha, 2008).

Warren and Root (1963) developed an idealized model in order to study the flow behavior in naturally fractured reservoirs. Their model assumes to contain an orthogonal system of continuous, uniform fractures which are parallel to the principal axes of permeability. The matrix is represented as discontinuous identical, rectangular parallelepipeds which are homogeneous and isotropic. The flow in this model only

occurs through fracture system with local fluid exchange with the matrix blocks. Fig.2.1 demonstrates the idealization of the fractured porous media.

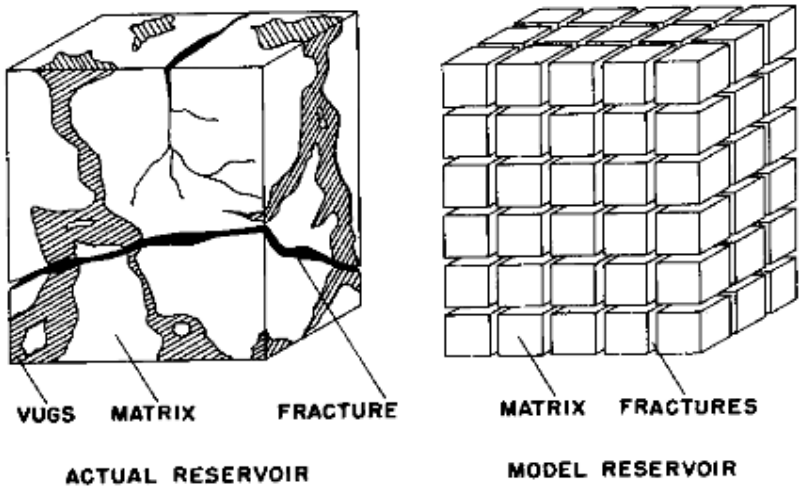

Fig. 2.1—Idealization of the naturally fractured reservoirs (Warren and Root, 1963)

The mathematical model for the single-phase fluid flow in homogeneous and anisotropic dual porosity reservoirs is described as (Warren and Root, 1963):

$$\frac{k_{fx}}{\mu}\frac{\partial^2 p_f}{\partial x^2}+\frac{k_{fy}}{\mu}\frac{\partial^2 p_f}{\partial y^2}-\phi_m C_m\frac{\partial p_m}{\partial t}=\phi_f C_f\frac{\partial p_f}{\partial t} \tag{2.1}$$

Subscript f represents the fracture porosity system, and m represents the matrix porosity system.

A quasi-steady state is assumed to exist in the matrix blocks. The mass balance equation within the matrix system is expressed as:

$$\phi_m C_m\frac{\partial p_m}{\partial t}=\frac{\sigma k_m}{\mu}(p_f-p_m) \tag{2.2}$$

σ was defined as a shape factor that describes the communication between fractures and matrix.

The single-phase dual porosity model is comprised of these two equations. Equation (2.2) is also treated as the transfer function, since no flow occurs between matrix blocks, which means the only flow exchange occurs in matrix system is through matrix and fractures. It is important to understand that the assumption of a quasi-steady state makes the solutions not accurate at early times. However, Warren and Root (1963) ultimately used the results in well testing, so the approximation in this case is adequate.

For uniformly spaced fractures, the shape factor can be simplified as:

$$\sigma = \frac{4n(n+2)}{l^2} \tag{2.3}$$

Kazemi et al. (1976) extended the single-phase flow equations derived by Warren and Root (1963) to multiphase flow in three dimensions. Their model accounts for imbibition, relative fluid mobility, gravity force, and variation in reservoir properties. Like the Warren and Root model, there are two flowing equations, one for fracture system, and another for matrix system.

$$\nabla \cdot \left[\lambda_{\alpha f} \rho_\alpha \nabla\left(P_{\alpha f} - \gamma_\alpha D\right)\right] - \tau_{mf} = \frac{\partial}{\partial t}\left(\phi_f \rho_\alpha S_{\alpha f}\right) \tag{2.4}$$

$$\tau_{mf} = \frac{\partial}{\partial t}\left(\phi_{ma} \rho_\alpha S_{\alpha ma}\right) \tag{2.5}$$

Here, $\alpha = w, nw$ represents wetting and non-wetting phases, respectively, f = fracture system, ma = matrix system. The transfer function τ_{mf} is defined as:

$$\tau_{mf} = k_{ma} V \sigma \lambda_{\alpha ma} \rho_{\alpha} \left[\left(P_{\alpha} - \gamma_{\alpha} D \right)_f - \left(P_{\alpha} - \gamma_{\alpha} D \right)_{ma} \right] \tag{2.6}$$

The material balance equation for a cubic matrix block is expressed as

$$\begin{aligned} &2k_{ma}\lambda_{\alpha}L_xL_y \frac{\left[\left(P_{\alpha} - \gamma_{\alpha} D\right)_f - \left(P_{\alpha} - \gamma_{\alpha} D\right)_{ma}\right]}{L_z/2} + 2k_{ma}\lambda_{\alpha}L_yL_z \frac{\left[\left(P_{\alpha} - \gamma_{\alpha} D\right)_f - \left(P_{\alpha} - \gamma_{\alpha} D\right)_{ma}\right]}{L_x/2} + \\ &2k_{ma}\lambda_{\alpha}L_xL_z \frac{\left[\left(P_{\alpha} - \gamma_{\alpha} D\right)_f - \left(P_{\alpha} - \gamma_{\alpha} D\right)_{ma}\right]}{L_y/2} = k_{ma}\lambda_{\alpha} V \sigma \left[\left(P_{\alpha} - \gamma_{\alpha} D\right)_f - \left(P_{\alpha} - \gamma_{\alpha} D\right)_{ma}\right] \end{aligned} \tag{2.7}$$

From the material balance equation stated above, the definition of their shape factor is given as,

$$\sigma = 4\left[\frac{1}{L_x^2} + \frac{1}{L_y^2} + \frac{1}{L_z^2}\right] \tag{2.8}$$

where L_x is the matrix block size not the grid block size.

As we notice, this mathematical model is simply a generalization of the single-phase model by replacing the pressure term with potential. This generalization has the build-in assumption that linear superposition of the two mechanisms-imbibition and gravity segregation is appropriate (Sarma 2003). In addition, the gridblock averaged saturation and potential are used in calculating transfer functions, since we can't get the saturation or pressure gradients at a smaller scale than the gridblock size. However, using gridblock average values in dual-porosity simulation will introduce some error to the solutions (Sarma 2003). To solve this, the matrix blocks may be required to further divided into sub-grid blocks to obtain a better definition of saturation distribution. However, this will increase the computational work dramatically, which may not be necessary.

Gilman and Kazemi (1983) continued to improve the dual porosity model by adding an upstream weighting factor ω in their transfer function.

$$\tau_{mf} = k_{ma} V \sigma \left(\lambda_{\alpha ma} \omega + \lambda_{\alpha f} (1-\omega)\right) \rho_\alpha \left[(P_\alpha - \gamma_\alpha D)_f - (P_\alpha - \gamma_\alpha D)_{ma} \right] \quad (2.9)$$

where $\omega = 1$ if flow is from matrix to fracture, = 0 if flow is from fracture to matrix. The shape factor is calculated using the same formula as in Kazemi's model. They noticed that the upstream weighting might not be appropriate, since saturation distributions cannot be found within the matrix block.

They've also noticed that within a given gridblock, the fluid height for the fractures and matrix may not be the same. Therefore, the term K_g was introduced to account for gravity forces in matrix-fracture fluid exchange.

$$D_{ma} = D_f + \Delta z \cdot K_g \quad (2.10)$$

Here K_g is a coefficient with a range from –0.5 to +0.5. By doing so, they made the gravity term saturation dependent. However, the use of phase density instead of density contrast makes the gravity term equal to zero, which is another shortcoming of this transfer function.

Thomas, Dixon and Pierson (1983) provided another version of the matrix/fracture transfer function in three-dimensional, three-phase dual porosity model, where the transfer function accounts for capillary pressure, gravity, and viscous forces. To include the effect of gravity forces, they used pseudo relative permeability and capillary pressure curves for both the matrix and fracture systems. However, the flow between fracture cells is calculated by using input capillary pressure curves. The effects

of pressure gradient across the matrix block and gas diffusion from saturated fracture to under-saturated matrix on matrix/fracture flow were represented by an extra source term in the transfer function.

In their model, the transfer term was defined as,

$$\tau_{mf} = 0.001127\sigma k_{r\alpha}\left(\frac{kV_b}{B_\alpha \mu_\alpha}\right)_m \left(P_m - P_f\right) \tag{2.11}$$

The value of shape factor in their single matrix block study was found to be process dependent and different from the one calculated using Warren and Root or Kazemi formula. An excellent agreement was achieved between the recoveries from the dual porosity model and the fine-grid model, when the shape factor equals to 25 (1 ft block) and 0.25 (10 ft block) in water/oil imbibition case, while equals to 2.0 (1 ft block) and 0.02 (10 ft block) in gas/oil case. These observations indicate that the Warren and Root and Kazemi formulas of shape factor lack in generality.

For fluid flowing from fracture to matrix, special considerations are given to upstream relative permeability which is maintained at matrix k_{rm} corresponding zero P_c, because flow is controlled by matrix properties. The matrix k_{rm} is multiplied by water saturation in fracture to account for fact that only the matrix blocks below the fracture water level will undergo imbibition.

$$k_{rw} = \left(k_{rw}\right)_{P_C=0} s_{wf} \tag{2.12}$$

And for oil relative permeability:

$$k_{ro} = \left(k_{rw}\right)_m s_{of} \tag{2.13}$$

Gas relative permeability is calculated as:

$$k_{rg} = \left(k_{rg}\right)_{(1-S_{org}-S_{wc})} S_{gf} \tag{2.14}$$

For fluid flow from matrix to fracture, matrix/fracture transfer function is evaluated using unaltered matrix relative permeability and capillary pressure values.

From their study, they concluded that the rate of recovery of oil and gas from a fractured reservoir was influenced by block size, wettability, and pressure and saturation history.

Further inclusion of the pressure gradient in matrix/fracture transfer function is defined as,

$$q_{\alpha mf} = \lambda_{\alpha}(P_{\alpha m} - P_{\alpha}) + \lambda_{\alpha} \frac{L_c}{L_B} \Delta P_{\alpha f} \tag{2.15}$$

where α = oil, water, L_B = distance over which ΔP acts, L_c = characteristic length.

Quandalle and Sabathier (1989) pointed out that the viscous forces, gravity forces and capillary forces in the matrix/fracture mass exchange are not equally affected. So they used three "flow coefficients" (κ_c, κ_g and κ_v) to adjust their relative effects on matrix/fracture transfer function by the following expression at point x+ :

$$\tau^{+}_{\alpha x} = 2K_{xma}\sigma_x \lambda_{\alpha x^+} \left[P_{ma} - P_f - \kappa_v \left(P_{fx^+} - P_f\right) + \kappa_c \left(P_{c\alpha oma} - P_{c\alpha of}\right)\right] \tag{2.16}$$

Equivalent formulas can be applied to the transfer function at points x-, y+, y-. However, at point z- the formula should include gravity forces:

$$\tau_{\alpha z}^{+} = 2K_{zma}\sigma_z\lambda_{\alpha z^+}\begin{bmatrix} P_{ma} - P_f + \kappa_v\left(P_{fz^+} - P_{fz} + \rho^* g(l_z/2)\right) \\ + \kappa_g\left[\left(\rho_{\alpha ma} - \rho^*\right)\cdot g\left(l_z/2\right)\right] + \kappa_c\left(P_{c\alpha oma} - P_{c\alpha of}\right) \end{bmatrix} \quad (2.17)$$

where $\rho^* = S_{wf}\rho_w + S_{of}\rho_o + S_{gf}\rho_g$, and shape factor is defined the same as that given by Kazemi et al.(1976) . An equivalent formula can be substituted for mass transfer at point z-.

However, they haven't given expressions for those three coefficients, which prohibits its further application in dual porosity simulator. For flow from fractures to matrix, they found that special consideration should be given to evaluate upstream relative permeability the same as in Thomas's model. They also pointed out that in the low fracture permeability case, the viscous effects in the transfer functions cannot be neglected.

Lim and Aziz (1995) derived the equation of matrix/fracture shape factor, which accounts for the transient pressure change in the matrix instead of making the pseudo-steady state assumption. Since the pressure diffusion dominates the flow mechanisms within matrix blocks, the single-phase shape factor was obtained by combining the analytical solutions of the pressure diffusivity equation with the mass balance equation of the matrix block. The single-phase matrix/fracture transfer function can be expressed as:

$$q = \frac{\pi^2}{L^2}\frac{\rho k}{\mu}(\overline{p_m} - p_f) \quad (2.22)$$

Here, the resulting shape factor is $\frac{\pi^2}{L^2}$ for one set fracture, $\frac{2\pi^2}{L^2}$ for two sets of fractures, and $\frac{3\pi^2}{L^2}$ for three sets of fractures.

It has been noted that although the derivation of shape factors is obtained without the assumption of pseudo-steady state, their shape factor equation is not accurate at early times as well due to the exponential approximation of the pressure diffusion solution they made in the derivation.

Even though significant progress has been made towards generating suitable matrix-fracture transfer functions in dual-porosity models, there are hardly any studies on transfer functions taking into consideration of vugs. This dissertation is an attempt to investigate the interaction between matrix, fractures, separate vugs and connected vugs with the final objective of understanding the complex mechanisms controlling the mass transfers to achieve transfer functions more representative of the naturally fractured, vuggy reservoirs.

2.2 Simulation Models for Naturally Fractured, Vuggy Reservoirs

The commonly used methods for modeling fluid flow through fractured, vuggy rock include: (1) dual-porosity models (Kossack et al., 2001, 2006), (2) multiple-continuum models (Abdassah and Ershaghis, 1986; Liu et al., 2003; Camacho-Velazquez et al., 2005; Wu et al., 2006), and (3) explicit discrete fracture-vug and matrix

models (Carlson et al., 1993, Parney et al., 2000, DeGraff et al., 2005, Dershowitz et al., 2007, Gulbransen et al., 2009, He et al., 2015).

Kossack, et al (2001, 2006) presented a numerical scale-up technique that creates a composite capillary pressure curve and a composite relative permeability curve, which incorporate the behavior of vugs in matrix system, to be incorporated in a dual porosity simulator, in order to give the same oil recovery as in fine-scale model. However, the highly heterogeneous nature makes vuggy media so unique that it cannot be incorporated into matrix porosity system.

A triple-continuum model was initially proposed by Abdassah and Ershaghis (1986) for the purpose of describing the anomalous slope changes in well tests of fractured reservoirs that could not be explained using dual-porosity models. Liu et al. (2003) later modified the triple-continuum model to describe single-phase fluid flow in fractured lithophysal reservoirs that contain fractures, rock matrices, and cavities. In their model, the shape factors for all three interporosity flows were evaluated using the Warren-Root pseudosteady-state model, the same as that utilized by Abdassah and Ershaghis (1986). Yu-Shu Wu et al. (2006) developed a triple-continuum conceptual model to study the multiphase flow behavior through vuggy fractured reservoirs. In their conceptual model, a great number of small or isolated cavities are included in the matrix system, while the vug system represents larger cavities that are directly or indirectly connected to overall fracture network through small fractures. However, the fracture-vug-matrix transfer functions in their model are just a general extension of matrix-fracture transfer function, without taking into consideration of the unique petrophysical

nature of vugs. Clearly, there is a strong demand to accurately model fractured, vuggy reservoirs based on the physics of the interaction among different porosity systems.

There have been some studies on using explicit discrete fracture-vug and matrix models to describe the flow behavior of naturally fractured, vuggy reservoirs. However, in those models, the number of grid blocks is too large for computers to handle, and therefore, flow problems may become computationally intractable for large scale models (Gulbransen et al., 2009). Arbogast et al. (2006) predicted that Darcy's law could be applied to the macroscopic modeling of naturally fractured, vuggy reservoirs over large scales. But, some type of upscaling is needed to emulate the flow behavior in the vugular heterogeneous porous media (Popov et al., 2007). Most upscaling techniques used effective macroscopic permeability that is derived through solving the mathematic models on the microscale within an upscaling coarse block (Arbogast et al., 2006, Popov et al., 2007, Gulbransen et al., 2009, Yan et al., 2013, 2015).

CHAPTER III

MATRIX-VUG TRANSFER FUNCTION

We have through the previous two chapters motivated the need for appropriate transfer functions to describe interporosity flows in the triple-continuum model. This chapter focuses on the fluid exchange between matrix and vug. It starts with an introduction of the conceptual models used in this study, follows by the development of the shape factor equation of single-phase flow, and ends up with a complete definition of the two-phase matrix-vug transfer function.

3.1 Conceptual Models of Fractured, Vuggy Formation

Naturally fractured, vuggy formation consists of multi-scale fractures, low permeability matrix, and spatially varying vugs. Vugs, which are void spaces created by diagenesis, can be a significant resource of hydrocarbon reserves. Depend on their location and connectivity to the overall fracture system, vugs are usually classified into two groups- isolated vugs and connected vugs. Isolated vugs are defined as vugs that is interconnected only through matrix. Most of them are small-sized vugs with diameters from millimeters to centimeters. Connected vugs are defined as vugs that are directly or indirectly connected to the global fracture network through small fissures or micro-fractures (Lucia, 1999, Jennings et al., 2001).

CT scans of the vuggy rock (**Fig. 3.1**) show a random distribution of isolated vugs at core scale. As we can see, vugs vary in size, shape and number within a certain

distance. **Fig. 3.2** shows the typical characteristics of fractured, vuggy reservoirs at field scale, with an overview of the complex connection between fractures, matrix and vugs of various sizes. Yu-Shu Wu (2006) conceptualized the fractured, vuggy formation as a multi-continuum system which consists of fractures, vugs, cavities and matrix in **Fig. 3.3**. Based on the unique features of fractured, vuggy rock shown in core and outcrop images, several conceptual models are established in **Fig. 3.4**. In those models, vug number and distribution are assigned randomly in matrix blocks. Fractures that connected to vugs vary in number and location with respect to the direction of the fluid flow (pressure gradient). For real reservoir models, the distribution and connectivity of vugs with respect to fractures may be determined by geo-statistical method.

The following discussions are only based on the models with isolated vugs, since this chapter only considers the mass transfer between matrix and vug. Oil in isolated vugs must first move to the matrix and then though matrix flow into the overall fracture system.

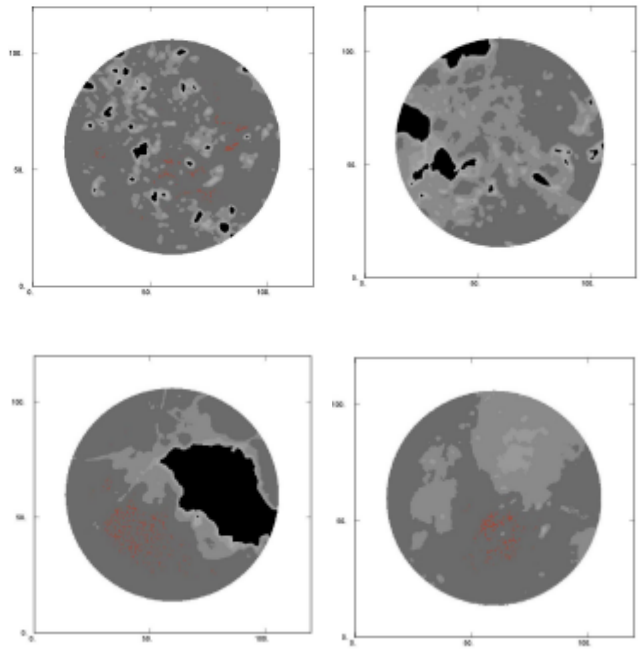

Fig. 3.1—Slide images of vuggy cores segments (Ricardo et al. 2000)

Fig. 3.2—Outcrop image of carbonate formation (Yu-Shu Wu et al, 2006)

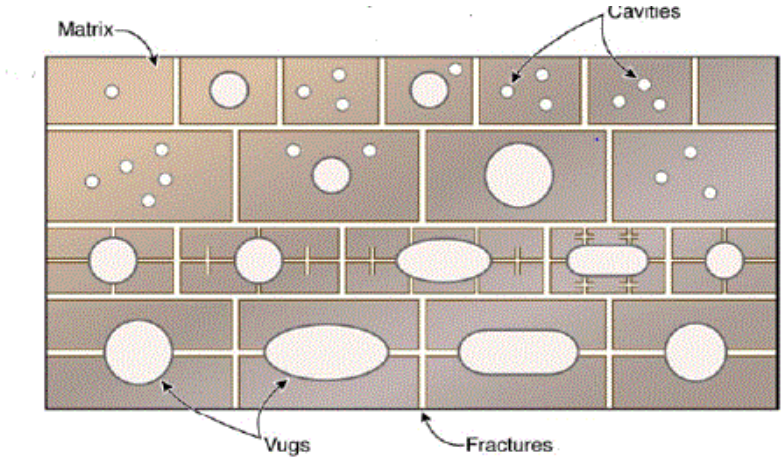

Fig. 3.3—Schematic of a multiple-continuum system used to describe fractured, vuggy formation (Yu-Shu Wu et al, 2006).

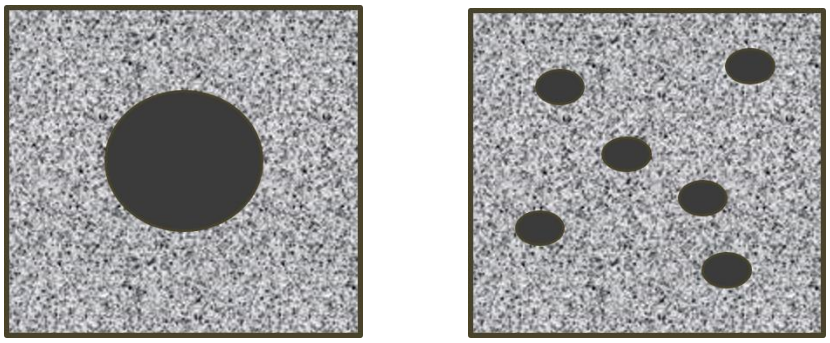

(a) Vug isolated from the global fracture network

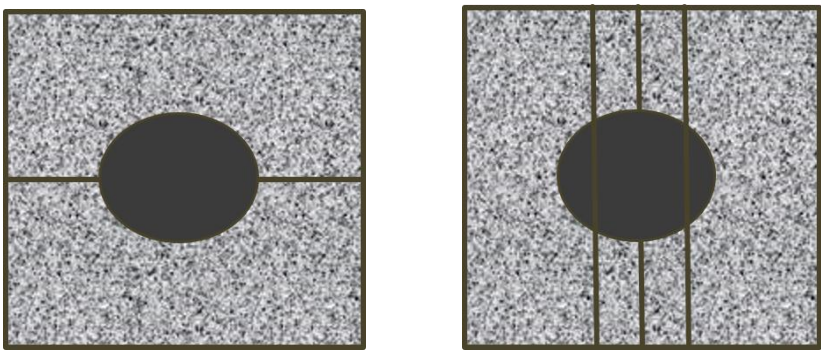

(b) Vug connected to the global fracture network

Fig. 3.4—Schematic of the conceptual models designed to be representative of fractured, vuggy rock

There has been some theoretical studies on modeling fluid flow through naturally fractured, vuggy reservoirs. And the practical and efficient approach to model such reservoirs has been through a triple-continuum model, where long-range fractures, low permeability matrix, random distributed vugs (isolated or connected to overall fracture network) are treated as three different continua with different petrophysical characteristics. The fracture system provides the path for global fluid flow, while vuggy and matrix continua mostly contributes to the fluid storage. Each porosity system interacts independently with the other two porosity systems. And the interporosity flows among them are represented by transfer functions. As illustrated in **Fig. 3.5**, in this study, 12×12×12 fine-grid blocks are upscaled into one coarse cell which has fracture, matrix and vug blocks superimposed on each other and located at the center of the coarse cell. In the following sections, we will propose appropriate transfer functions to describe the flow between matrix system and vug system as well as the flow between fracture system and vug system.

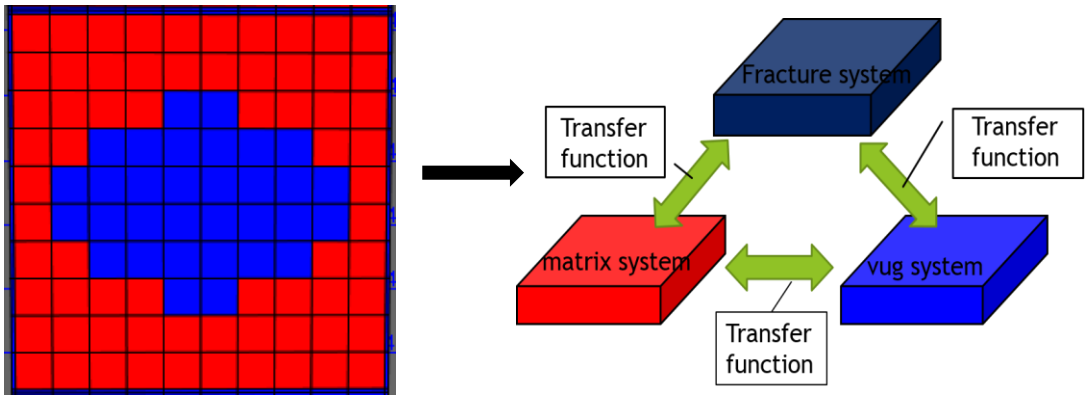

Fig. 3.5—Schematic of fine-grid model vs. triple-continuum model from simulation perception

3.2 Single-phase Matrix-vug Transfer Function

3.2.1 Mechanisms of Single-phase Mass Transfer

For single-phase flow, the mechanisms of mass transfer between matrix and vug include fluid expansion and viscous displacement. In most cases, fluid expansion will be the dominating mechanism.

General form of single-phase matrix-vug transfer function is given as:

$$\Gamma_{mv} = \sigma \frac{k}{\mu}(\Phi_v - \Phi_m) \tag{3.1}$$

Here, σ is shape factor, also called geometric shape factor, account for the geometric part of interporosity flow behavior. The general form of shape factor for matrix and fracture transfer function is given by a/L^2, where a is a constant that has been given different values in various dual porosity models discussed in the previous chapter. The formula of shape factor in matrix-vug transfer function will be developed in next section.

3.2.2 The Effect of Vug Spatial Variation

Vugs in conceptual models vary in size, shape and distribution. This spatial variation affects the flow behavior when initial oil in vugs flows into outside matrix. Therefore, different concept models of vug filled matrix blocks (surrounded by fractures on all sides) were generated to study the effect of vug spatial variation on fluid flow behavior.

First, fine-grid, single porosity models with vug fraction increased from 3.20% to 20.00% were built to evaluate the effect of vug fraction on oil recovery from vugs. See

Fig. 3.6 for the representation of fractures, matrix and vugs in fine-grid model, where blue area represents the vug, and red area represents matrix, which is surrounded with fractures on all the six sides. Subjected to the same pressure drawdown, the oil recovery curves corresponding to five different vug fractions are plotted in **Fig. 3.7**. As can be seen, for a reservoir with lower vug fraction, the oil recovery rate is faster. Therefore, vug fraction should be taken into consideration when investigating the mass transfer between matrix and vug.

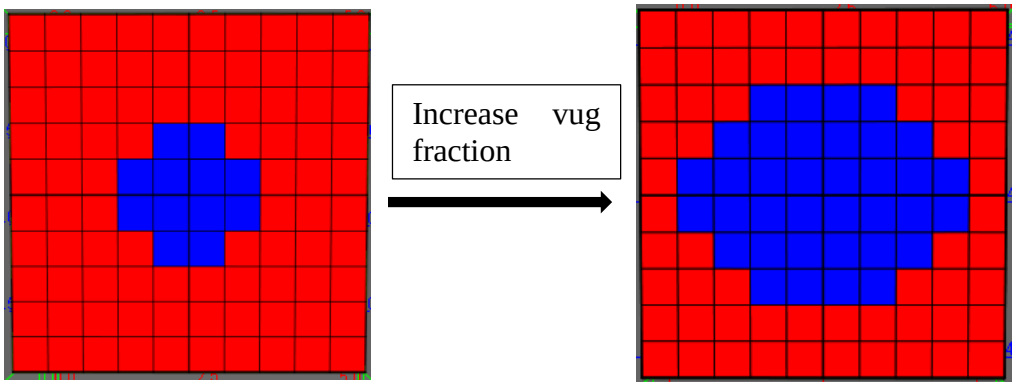

Fig. 3.6—X-Z cross-section of fine-grid, single porosity simulation model with the increase of vug fraction (blue areas correspond to vugs)

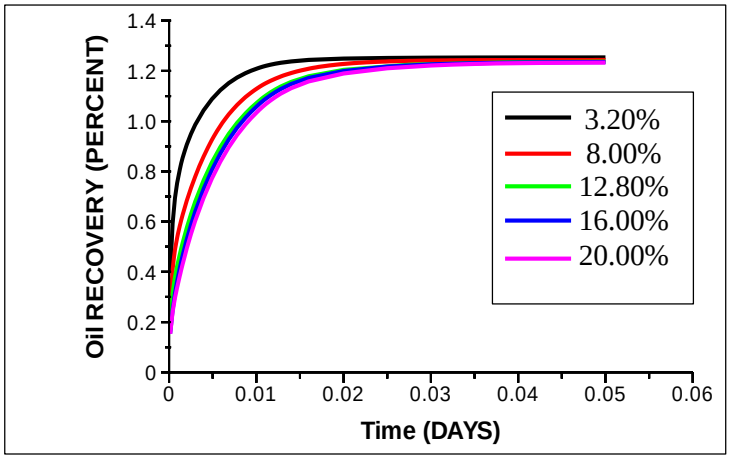

Fig. 3.7—Total oil recovery vs. time from fine-scale simulation: sensitivity to vug fraction

In the next step, with the same vug fraction, vug number is increased from one to maximum (the maximum number is reached by dividing the vug pore volume by fine-grid block volume) to study its effect on flow behavior. **Fig. 3.8** shows the designed simulation models that have the same vug fraction but different vug number, which also gives different vug size. The result in **Fig. 3.9** shows that as the vug number increases, the rate of oil recovery increases. A clear difference between the oil recovery curve of single-vug case and two-vug case is observed in **Fig. 3.9**, while the oil recovery curve of two-vug case is very close to the one has maximum vug number. So in the next section, three different scenarios - single-vug, two-vug, and vugs of maximum number - are investigated separately. Any vug numbers fall within two to the maximum number, we use average to get the shape factor value.

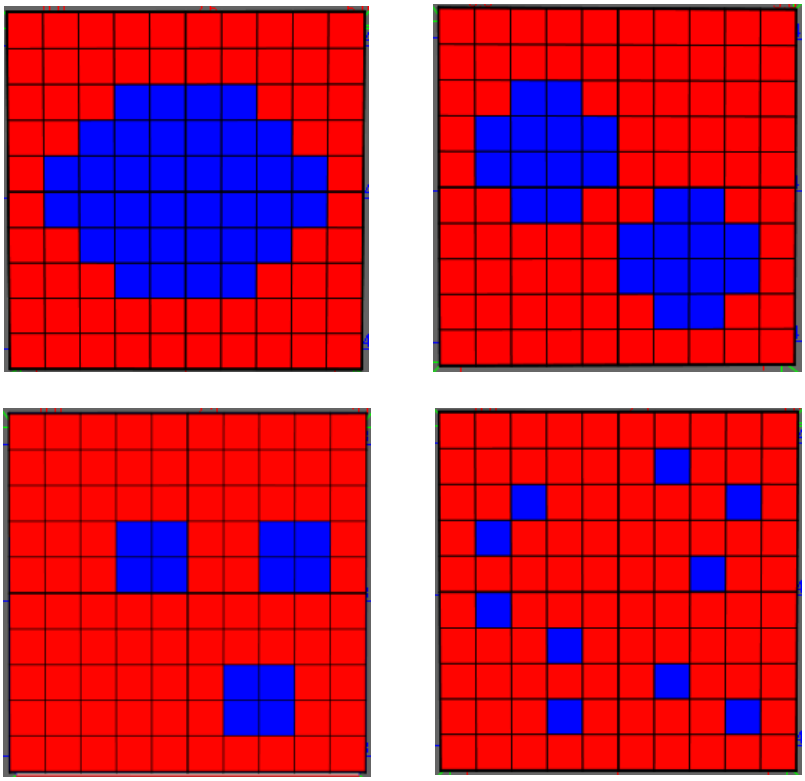

Fig. 3.8—X-Z cross-sections of fine-grid, single porosity simulation models with increased number of vugs

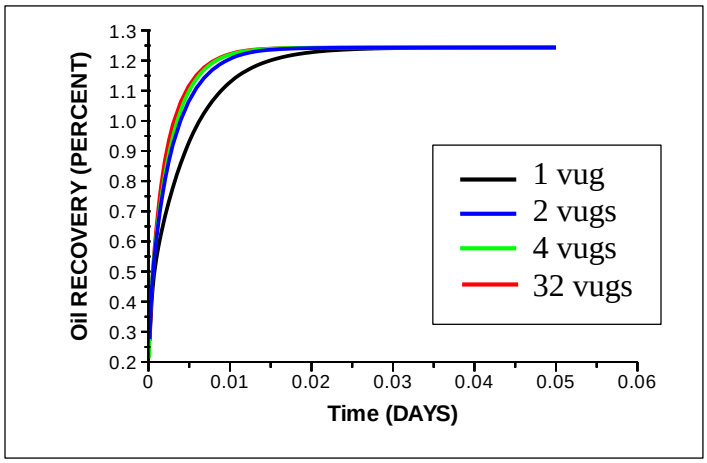

(a) Vug fraction = 3.20%

Fig. 3.9—Total oil recovery from fine-grid, single porosity models: sensitivity to number of vugs

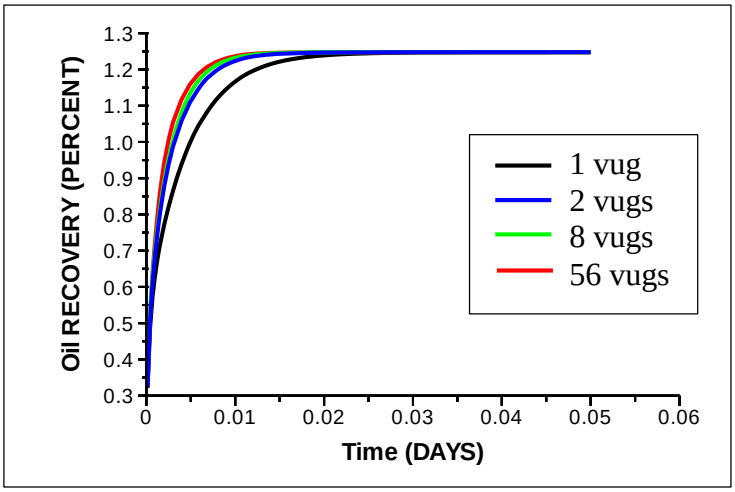

(b) Vug fraction = 5.60%

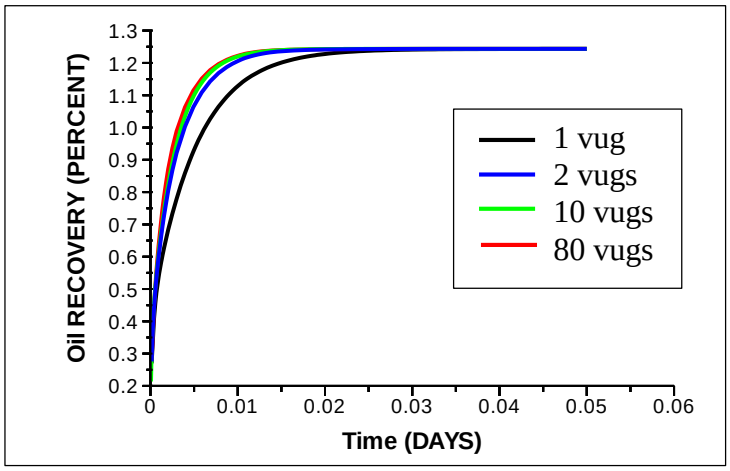

(c) Vug fraction = 8.00%

Fig. 3.9—Continued

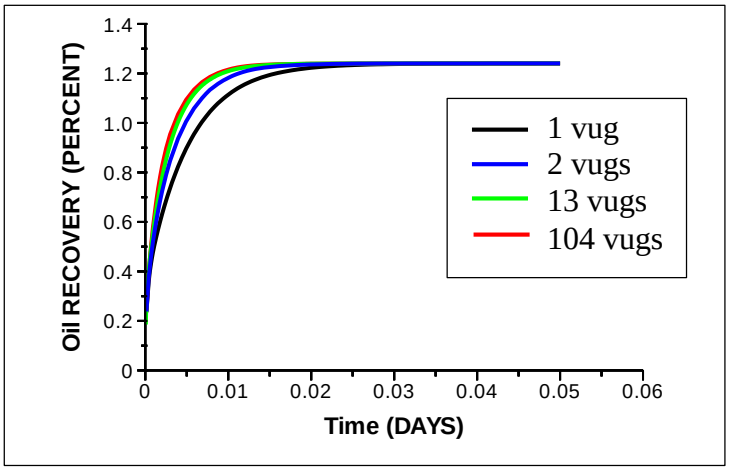

(d) Vug fraction = 10.4%

Fig. 3.9—Continued

3.2.3 Shape Factor

Coarse models are built on a commercial reservoir simulator where fractures, matrix, and vugs are considered as three different flowing systems. The porosity and permeability were adjusted so that the matrix block, fracture block and vug block in the coarse model have the same pore volume and flowing capacity as in the fine-grid model. By changing the value of shape factor, a good agreement between the fine-grid model solutions and the coarse model results is obtained. An example is shown in **Fig. 3.10**. As mentioned in last section, cases with different vug numbers - single, two and the maximum number - are discussed separately, each with realizations of various vug fractions and grid block sizes. The history matching results for single-vug case are summarized in Table 3.1. A correlation of the shape factor with $F_v \frac{1}{L_x^2}$ for single-vug case is plotted in **Fig. 3.11**.

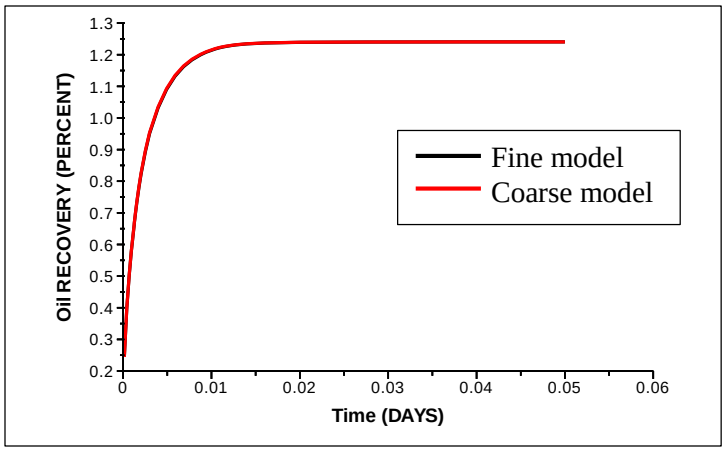

Fig. 3.10—Total oil recovery vs. time of the fine-grid, single porosity model matching with the tripe-continuum model (vug fraction=10.4%)

Table 3.1—Shaper factor for cases with different vug fraction and grid block size (single-vug case)

Vug fraction	Lx	1/Lx/Lx	Fv/Lx/Lx	Shape Factor
0.032	3	0.11	0.00351	0.33
0.032	4	0.06	0.00198	0.19
0.032	5	0.04	0.00127	0.12
0.032	8	0.02	0.00050	0.045
0.056	3	0.11	0.00611	0.58
0.056	4	0.06	0.00345	0.33
0.056	5	0.04	0.00221	0.21
0.056	8	0.02	0.00087	0.08
0.08	3	0.11	0.00871	0.83
0.08	4	0.06	0.00493	0.47
0.08	5	0.04	0.00316	0.29
0.08	8	0.02	0.00124	0.12
0.104	3	0.11	0.01131	1.1
0.104	4	0.06	0.00639	0.61
0.104	5	0.04	0.00411	0.4
0.104	8	0.02	0.00161	0.155
0.128	5	0.04	0.00504	0.455
0.144	5	0.04	0.00569	0.55
0.16	5	0.04	0.00630	0.59
0.2	5	0.04	0.00786	0.75
0.23	5	0.04	0.00912	1.00
0.302	5	0.04	0.01192	1.40

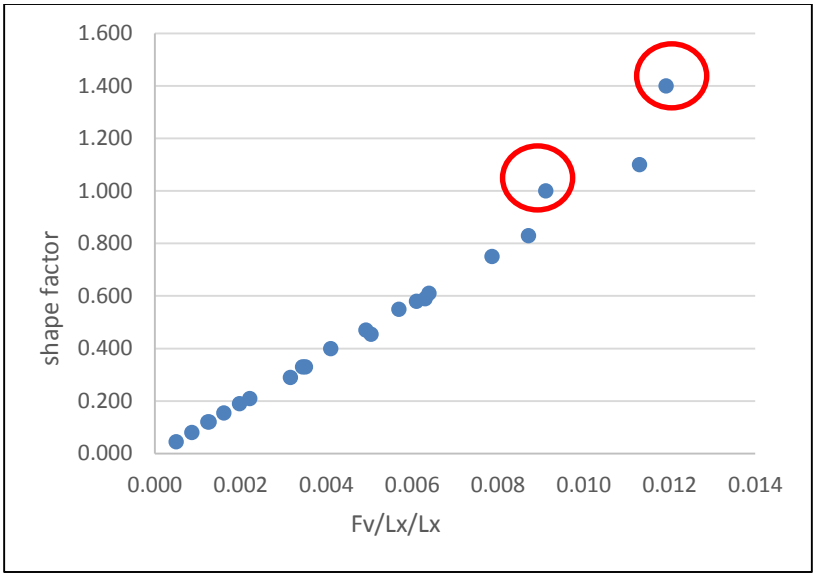

Fig. 3.11—Shape factor vs. $F_v \frac{1}{L_x^2}$ (single-vug case)

As can be seen, two points with vug fraction greater than 20% deviate from the straight line, so the developed shape factor equation only apply to the vug fraction less than 20%, which is applicable, since most vug fractions in literature were found to be less than 20%. By eliminating these two points, a linear relationship between shape factor and $F_v \frac{1}{L_x^2}$ can be reached at

$$\sigma = 96 F_v \frac{1}{L_x^2} \tag{3.2}$$

Fig. 3.12 shows the linear relation between shape factor and $F_v \frac{1}{L_x^2}$ within 20% vug fraction for single-vug case.

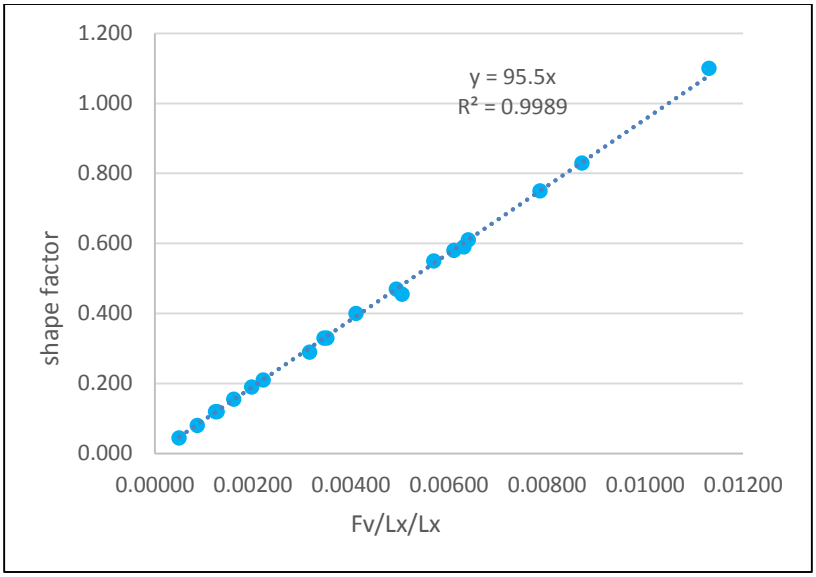

Fig. 3.12—Shape factor vs. $F_v \frac{1}{L_x^2}$ within 20% vug fraction (single-vug case)

Following the same procedure, **Fig. 3.13** shows the linear relation between shape factor and $F_v \frac{1}{L_x^2}$ for two-vug case. And after linear regression, the shape factor for two-vug case can be expresses as:

$$\sigma = 173 F_v \frac{1}{L_x^2} \tag{3.3}$$

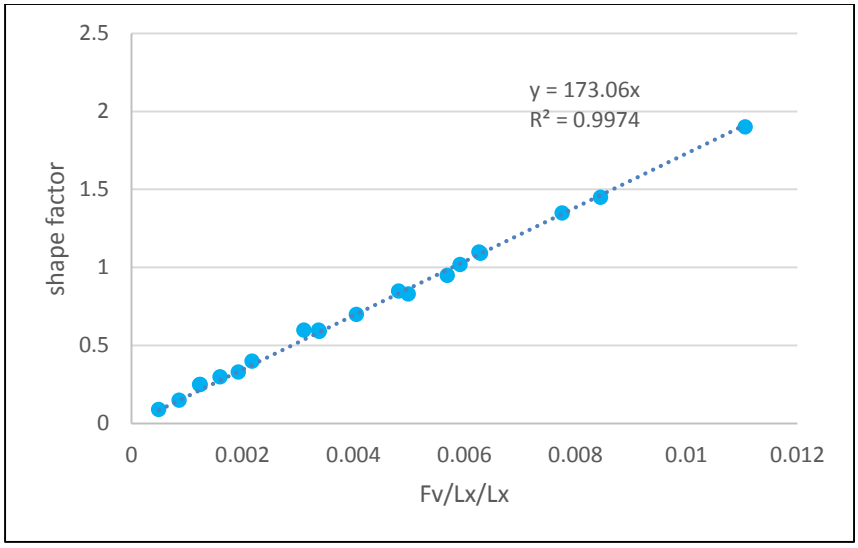

Fig. 3.13—Shape factor vs. $F_v \frac{1}{L_x^2}$ (two-vugs case)

Fig. 3.14 shows the linear relation between shape factor and $F_v \frac{1}{L_x^2}$ for the case with maximum number of vugs. Linear regression is used to get the shape factor equation for the case with maximum number of vugs as:

$$\sigma = 305 F_v \frac{1}{L_x^2} \tag{3.4}$$

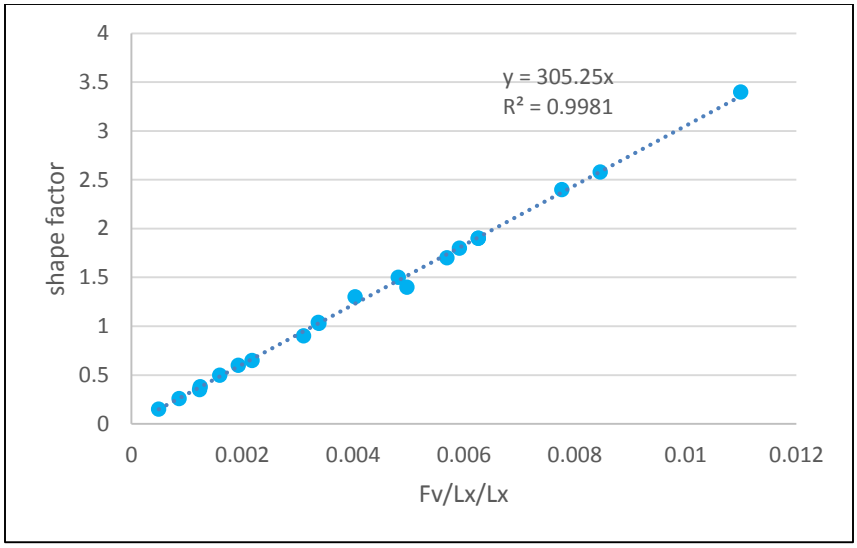

Fig. 3.14—Shape factor vs. $F_v \frac{1}{L_x^2}$ (case with maximum number of vugs)

As can be seen, the coefficient in the shape factor equation increases as the number of vugs in the representative model increases. That's because the contact area between matrix and vug increases with the increase of the number of vugs in the representative model. These linear correlations developed on the basis of history matching allows the estimation of the shape factor in single-phase matrix-vug mass transfer.

3.3 Dynamic Matrix-vug Transfer Function

3.3.1 Model Introduction

The main objective of this research is to determine the interporosity transfer functions so that one can use triple continuum models to simulate naturally fractured,

vuggy reservoirs on the coarse scale. This section will propose a well-designed process to develop the matrix-vug transfer function. The whole process is conducted on a commercial reservoir simulator.

First, a three dimensional two-phase fine-scale, single porosity simulation model is introduced to provide a benchmark for triple continuum models. In this model, a vug filled matrix block 5.0 feet cube is divided into 10×10×10 grid blocks. After adding fractures of 0.01 feet thickness on all six sides of the matrix block, the model has 12×12×12 grid blocks. See the left part of **Fig. 3.15** for the cross-section of this 3D fine-grid model. The porosities of matrix, fractures, and vugs are assigned as $\phi_m = 0.06$, $\phi_f = 1.0$, and $\phi_v = 1.0$ respectively. And the permeabilities of matrix, fractures, and vugs are assigned as $k_m = 0.1mD$, $k_f = 5000mD$, and $k_v = 20000mD$ respectively. Matrix relative permeability curve and capillary pressure curve are shown in **Fig. 3.16** and **Fig. 3.17.** Straight-line relative permeabilities and zero capillary pressure are assigned to the fractures and vugs. The number of vug grid blocks should be corresponding to the vug fraction which is varied by cases from 3.2% to 20.0%. Special attention should be given to the locations of vug grid blocks which is required to be isolated by matrix grid blocks from fractures, because here we only consider isolated vugs. At the top and bottom of the representative model, additional layers of fracture grid blocks are added for well connections. Twelve water injection wells, with twelve connections each, are located on the bottom fracture grid blocks. The injection rate can be vary to give a different pressure gradient across the representative model. Twelve

production wells are placed on the top of the model. Bottom-hole pressure is maintained at 4700 psi. Initial reservoir pressure is 4800 psi. The oil recovery as a function of time was recorded until the time when maximum oil recovery is reached.

Next, a triple porosity simulation model of factures, matrix and vugs should be established to match the results of the fine-grid model. This model represents factures, matrix and vugs using three grid blocks superimposed on each other shown in the right part of **Fig. 3.15**. The porosities of fracture, matrix and vug grid blocks are recalculated to match the corresponding pore volumes in the single porosity, fine-grid model. An injection well and a production well should be placed on the extra fracture grid blocks which are on the top and bottom of the representative cell. These two wells run under the same schedule as they were in the fine-grid simulation. The total oil recovery is recorded and compared with the one got from the single porosity, fine-grid model. The goal here is to create a pseudo capillary pressure for the vug system so that the triple continuum model can match the results of the fine-grid model.

Finally, models of different vug fractions and distributions are created, and then the procedure is repeated until all the models have been matched. The final form of matrix-vug transfer function will be given by summarizing the pseudo capillary pressure of vug system for all models.

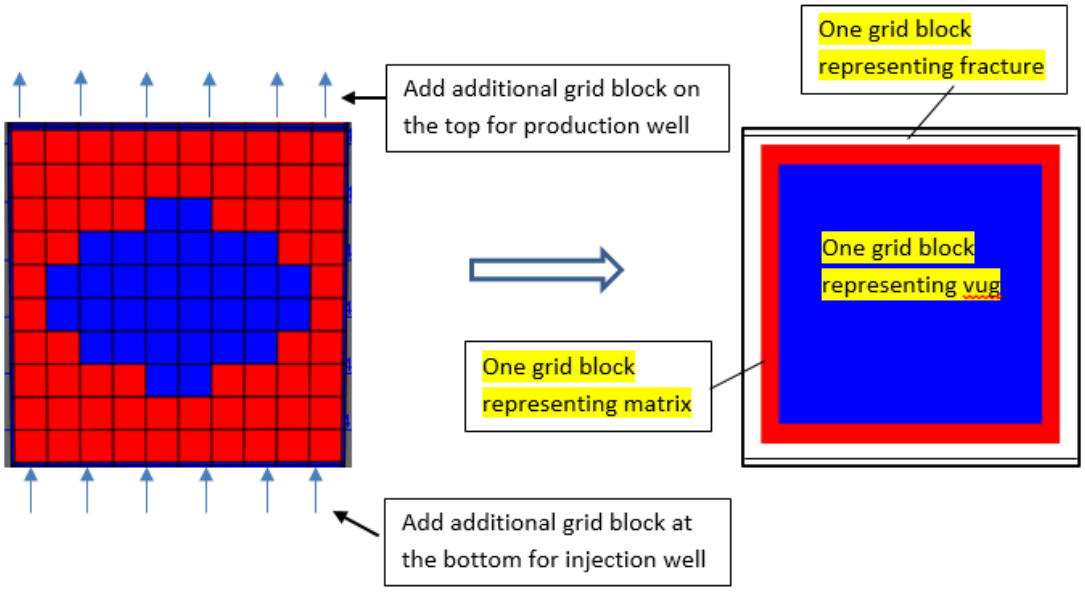

Fig. 3.15—Schematic of the simulation process with cross-sections showing the fine-grid model and the corresponding coarse model

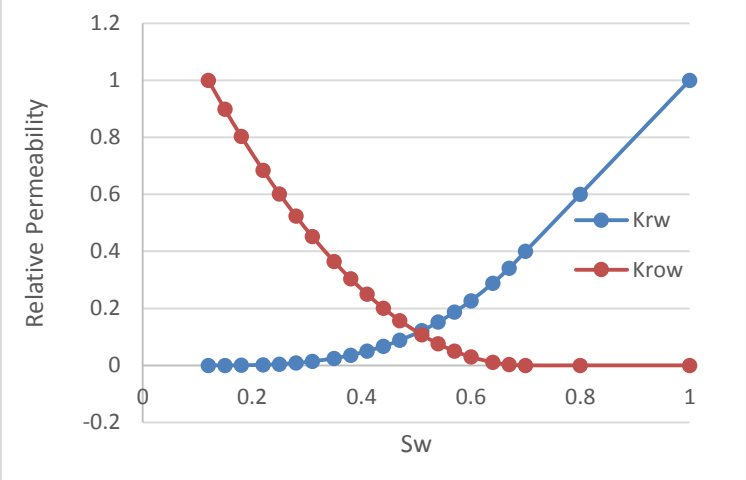

Fig. 3.16—Relative permeability curve for matrix rock

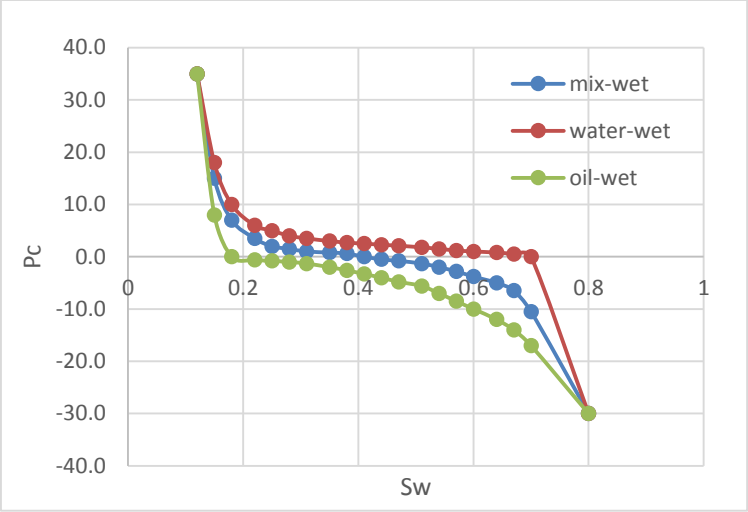

Fig. 3.17—Capillary pressure curve for matrix rock

3.3.2 Two-phase Matrix-vug Mass Exchange Mechanisms

The mass transfer mechanisms of a triple continuum model with multiphase flow include viscous force, capillary force, gravity, fluid expansion and mass diffusion. For oil-water cases, the diffusion of components from one phase to another can always be neglected (Kossack et al. 2001). The dominant forces for most naturally fractured, vuggy reservoirs are viscous force, capillary force and fluid expansion. Gravity may have a great influence on mass transfer for some cases. Next, we will discuss how these forces work together to displace oil from vugs. We will also investigate the sensitivity to the following parameters: wettability, density difference, vug shape, pressure gradient, and minimum capillary pressure. This choice is no arbitrary, as these parameters correspond to the magnitude of forces acting on the fluid exchange.

Fractures, matrix and vugs are initially saturated with oil. As water injected into the system, the invasion of fractures by water happens very fast due to the high

permeability of fracture system, and then water starts flowing into matrix and replacing oil from the matrix system. When the water saturation in matrix reaches a certain level, water starts entering into vugs from side or bottom matrix grid blocks or both as illustrated in **Fig. 3.18**.

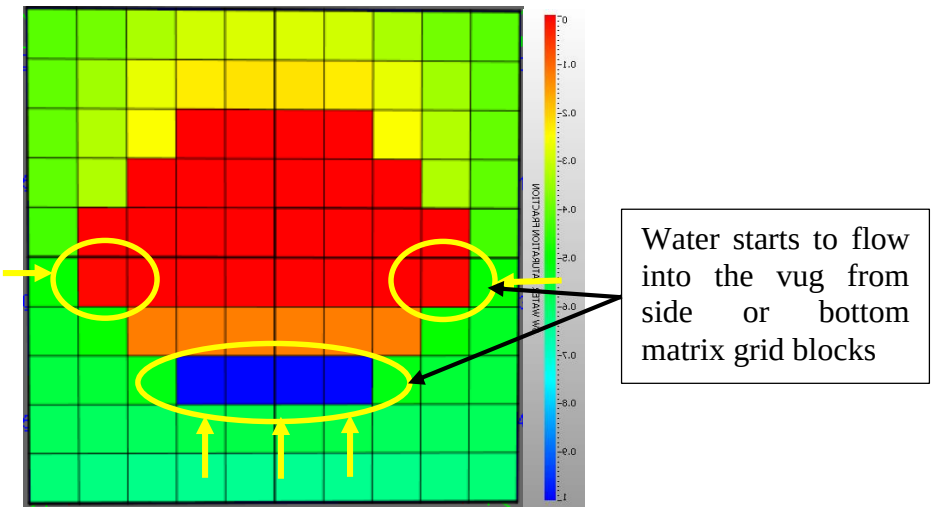

Fig. 3.18—Saturation profile of the fine-grid, single porosity representative model in the early times

In water wet cases, the capillary pressure will oppose the fluid exchange between matrix and vugs. However, the effect of capillary force will decrease as the water saturation in matrix increases. In the lower part of vugs, the pressure of vug grid blocks are always lower than the pressure of their surrounding matrix grid blocks, contributing to the mass exchange between matrix and vugs. The gravity force acts as a driving force in oil displacement from vugs.

In oil wet cases, the capillary pressure will help drive water from matrix into vugs. And as the production time goes on, the capillary force increases, becoming the

dominating force in the later times. In the early times, the pressure of lower part of vugs is less than its surrounding matrix grid blocks. But as the water saturation of vugs increases, that pressure increases and finally becomes higher than the pressure of its surrounding matrix grid blocks. The gravity force works in the favor of an upward displacement of oil in vug system.

In mix wet cases, capillary pressure will inhibit the fluid exchange between matrix and vugs in the early times, and later contribute to the oil displacement in vugs. The change of pressure difference between vug grid blocks and surrounding matrix grid blocks are following the same trend as in oil wet cases. The gravity force drives the oil displacement from vugs. A comparison of the average pressure of vug system and matrix system in water wet, oil wet and mix wet cases is shown in **Fig. 3.19**.

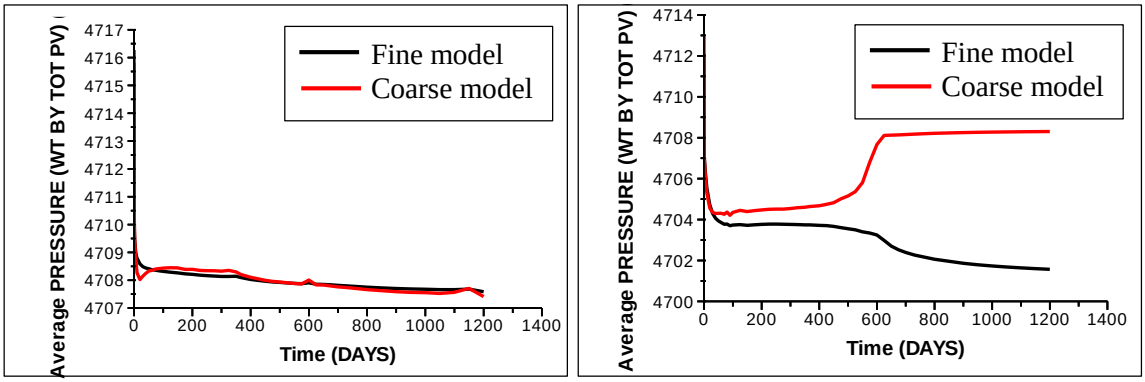

(a) Water wet **(b) Oil wet**

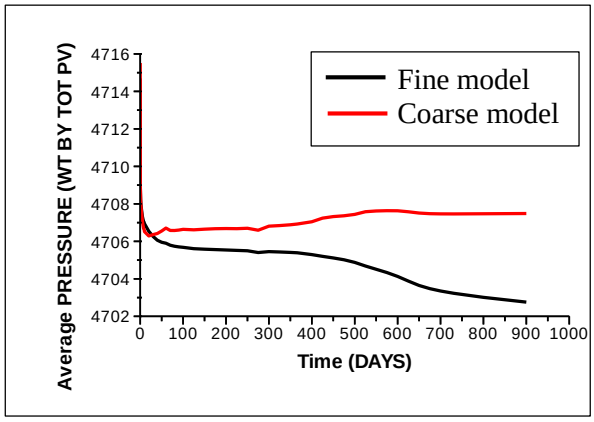

(c) Mix wet

Fig. 3.19—Comparison of the average pressure of vug system and matrix system

Effect of wettability

As shown in **Fig. 3.20**, the final recovery of the water wet case is the highest among three different wettability cases, because it has the highest water saturation in matrix, and oil can be recovered 100% from vug system in all the three cases. In the early times, water can easily flow into matrix in the water wet case, so oil recovery is higher than those in oil wet case and mix wet case. However, because capillary force acts as a counterforce to fluid exchange in the water wet case, the oil recovery rate is

slower than the other two cases, resulting in oil recovery falling below the other two cases at the intermediate times. At the end, the final oil recovery of water wet case will reach the highest again.

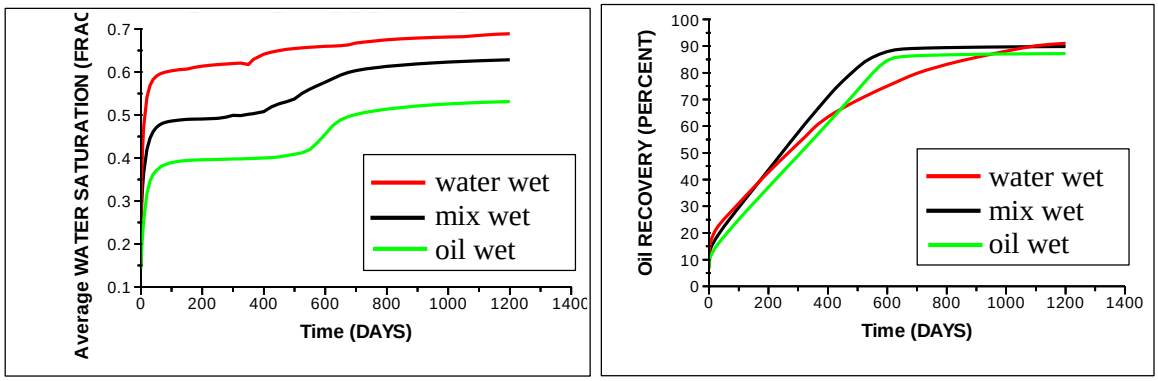

(a)Water saturation in matrix system **(b) Total oil recovery**

Fig. 3.20—Sensitivity to wettability

Effect of fluid density difference

As shown in **Fig. 3.21**, the final recovery of the case with oil density of 31.8 lb/ft^3 is slightly higher than those of 47.2 lb/ft^3 and 56.8 lb/ft^3. Because the case with higher density difference has a larger gravity force that helps to drive the water from fracture into matrix, and with the increase of matrix water saturation, capillary pressure will rise to help drive the water into vugs. On the other hand, gravity force that helps to displace oil in vug system will also increase due to the density difference. But as we calculate the gravity force using Equation (3.5), the value turns out to be very small in this case, which corresponding to the results shown in **Fig. 3.21**.

$$P_g = \Delta\gamma \bullet g / g_c \bullet \Delta H \tag{3.5}$$

Here, $g / g_c = 0.0069444(lb \cdot ft^2 / lb \cdot in^2)$.

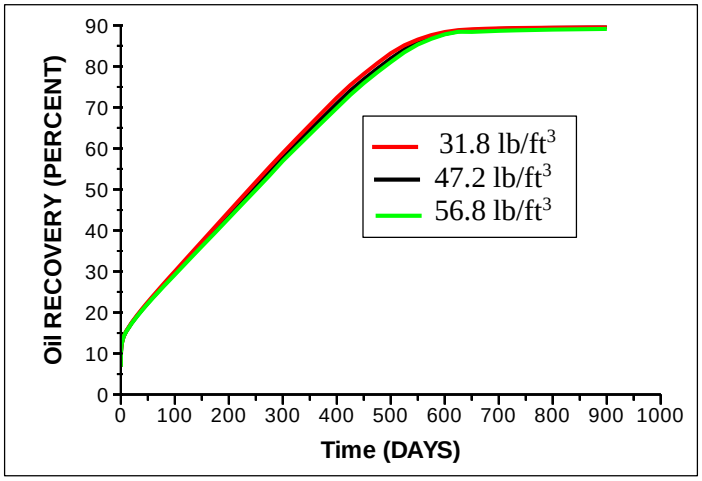

Fig. 3.21—Sensitivity to density difference

Effect of vug shape

When the vug number per coarse cell increases, the vug size becomes smaller. See the different vug shapes in **Fig. 3.22**. As show in **Fig. 3.23**, the bigger vug shape with higher vug height leads to a higher oil recovery. This is mainly caused by the fact that the pressure difference across the vug increases when the vug height (more accurately, the vug length along pressure gradient) increases.

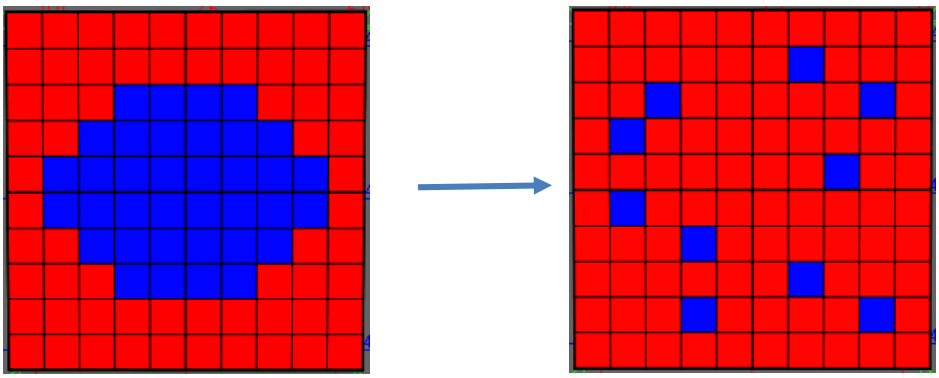

Fig. 3.22—Cross-section of models with different vug shape

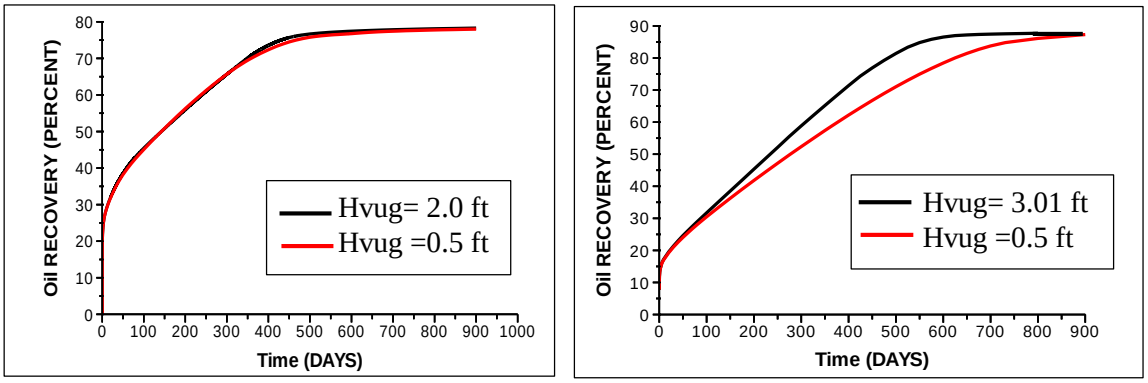

(a) Vug fraction of 3.21% **(b) Vug fraction of 10.39%**

Fig. 3.23—Sensitivity to vug shape (represented by vug height)

Effect of injection rate

As shown in **Fig. 3.24**, oil recovery becomes faster as the injection rate increases, because the pressure gradient across the vug is higher for cases with higher injection rate.

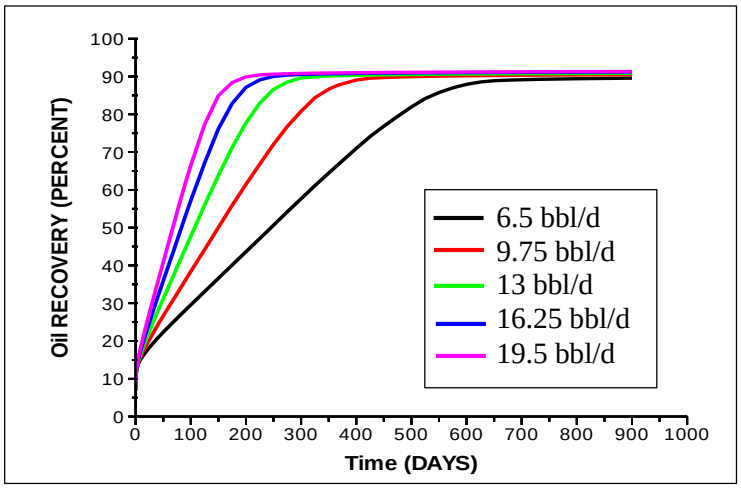

Fig. 3.24—Sensitivity to injection rate

Effect of capillary pressure

Four capillary pressure curves with different minimum values are displayed in **Fig. 3.25**. **Fig. 3.26** shows total oil recovery curves corresponding to the four capillary pressure curves. Among them, the case with the lowest value of minimum capillary pressure shows the lowest oil recovery rate. Because in the case with lower capillary pressure, water in the vugs, instead of going upwards，tends to flow back to the matrix.

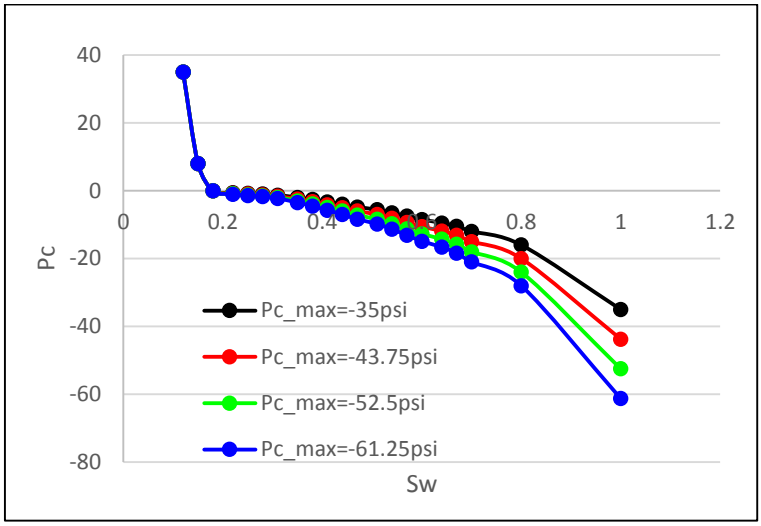

Fig. 3.25—Capillary pressure for matrix rock

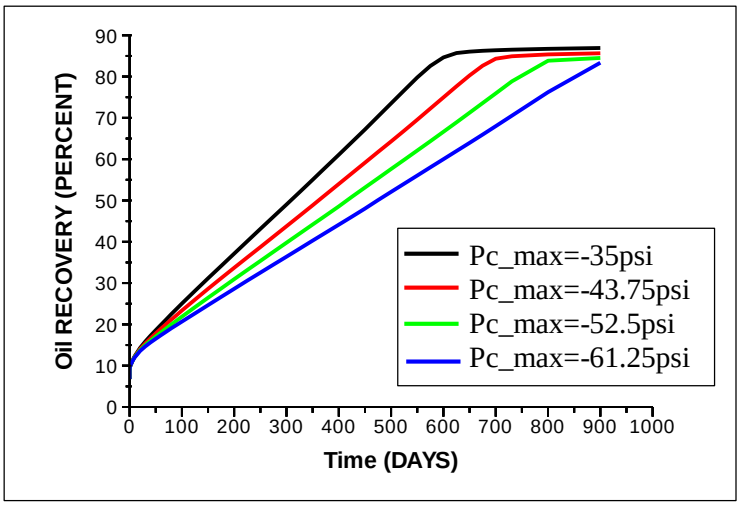

Fig. 3.26—Sensitivity to capillary pressure

According to the sensitivity analysis results, conclusions can be summarized as listed below.

1. The fluid exchange between matrix and vug is largely affected by rock and fluid characteristics and saturation history. For matrix with different wettabilities or capillary pressure curves, the transfer functions between matrix and vug should be different.
2. Gravity has a minor effect on mass exchange between matrix and vugs. However, this may not be the case for vugs with significant heights.
3. As the pressure gradient increases, the viscous force acting on the fluid exchange between matrix and vugs increases, which helps to enhance the speed of oil displacement from vug system.
4. The developed matrix-vug transfer function should incorporate all the mechanisms discussed above.

3.3.3 Dynamic Matrix-vug Transfer Function

For two-phase, 3D flow in triple porosity reservoirs, the mass balance equation in fracture domain can be expressed as

$$\nabla \cdot \left[T_{\alpha f} \nabla (p_{\alpha f} - \gamma_\alpha D)\right] + \Gamma_{mf} + \Gamma_{fv} - q_\alpha = \frac{\partial}{\partial t}\left(\phi_f \rho_\alpha S_{\alpha f}\right) \tag{3.6}$$

In matrix domain,

$$\nabla \cdot \left[T_{\alpha m} \nabla (p_{\alpha m} - \gamma_\alpha D)\right] - \Gamma_{mf} + \Gamma_{mv} = \frac{\partial}{\partial t}\left(\phi_m \rho_\alpha S_{\alpha m}\right) \tag{3.7}$$

In vug domain,

$$\nabla \cdot \left[T_{\alpha v} \nabla (p_{\alpha v} - \gamma_\alpha D)\right] - \Gamma_{mv} - \Gamma_{fv} = \frac{\partial}{\partial t}\left(\phi_v \rho_\alpha S_{\alpha v}\right) \tag{3.8}$$

Here, α is the phase (= oil or water), Γ_{mf} , Γ_{mv} and Γ_{fv} are the mass transfer terms between three flowing domains. In this section, only isolated vugs are considered, so $\Gamma_{fv} = 0$.

The transfer function between matrix and vug can be expressed as:

$$\Gamma_{mv} = \sigma \frac{k}{\mu}(\Phi_v - \Phi_m) \tag{3.9}$$

In Quandalle&Sabathier (1989) transfer function, three "flow coefficients" (κ_c, κ_g and κ_v) were used to adjust the relative effects of three active forces (viscosity, gravity, and capillarity) on fluid exchange between matrix and fracture. An extension was made to describe the transfer function between matrix and vug by replacing the

potential term with forces acting on matrix/vug fluid exchange. At point x+, the fluid exchange can be expressed as

$$\Gamma_{\alpha x}^{+} = 2K_{xm}\sigma_x\lambda_{\alpha x^+}\left[P_m - P_v + \kappa_v\left(P_{mx^+} - P_{mx}\right) + \kappa_c\left(P_{c\alpha om}\right)\right]$$

(3.10)

Equivalent formulas can be applied to describe fluid exchange at point x^-, y^+ and y^-, while at point z^+ (or z^-), the fluid exchange formula is given as

$$\Gamma_{\alpha z}^{+} = 2K_{zma}\sigma_z\lambda_{\alpha z^+}\begin{bmatrix} P_m - P_v + \kappa_v\left(P_{mz^+} - P_{mz} + \rho_\alpha^m g(l_z/2)\right) + \\ \kappa_g\left[\rho_\alpha^m g(l_z/2) - \rho^* g\left(l_v/2\right)\right] + \kappa_c\left(P_{c\alpha om}\right) \end{bmatrix} \quad (3.11)$$

Here, $\rho^* = S_{wv}\rho_w + S_{ov}\rho_o$.

A simplification was made on this transfer function by introducing a pseudo capillary pressure for vug system. The simplified transfer function is expressed as

$$\Gamma_{\alpha mv} = \sigma k_m \lambda_{\alpha m}(\Phi_v - \Phi_m) = \sigma k_m \lambda_{\alpha m}(P_v - P_{cap\_v} - P_{\alpha m}) \quad (3.12)$$

A comparison of these two transfer functions shows that, the developed pseudo capillary pressure should account for the viscous force and gravity force in fluid exchange. **Fig. 3.27** shows a good matching results of oil recovery from the fine-scale simulation model and the triple-porosity, coarse simulation model, by adding a pseudo capillary pressure for vug porosity system (Table 3.2).

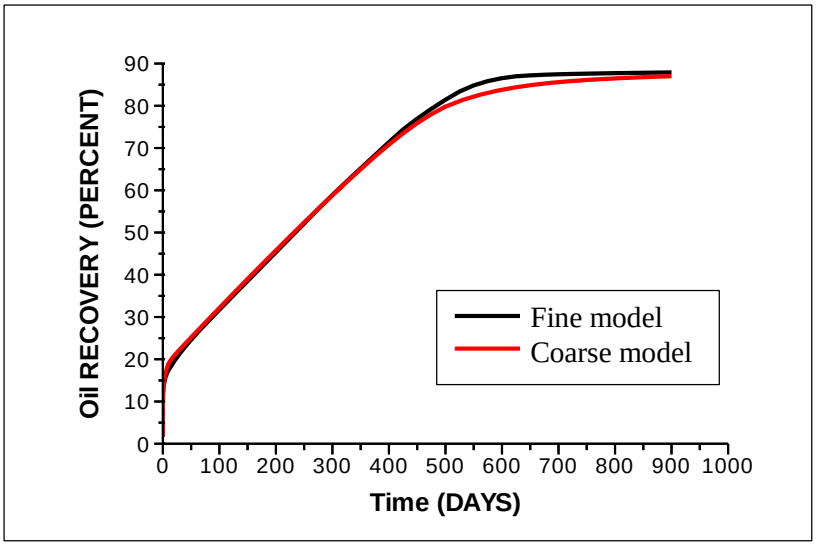

Fig. 3.27—Oil recovery vs. time for fine-grid, single porosity simulation and triple porosity simulation

Table 3.2—Pseudo capillary pressure for vug system

SW	KRW	KROW	PCWO
0	0.000	1.000	5.5
1	1.000	0.000	5.5

It is observed that the value of pseudo capillary pressure of vug system is constant. To determine its value, we design models with various vug fraction, vug distribution and injection rate. The choice of these variables is no arbitrary, since these parameters will influence the effects of viscous force and gravity force on fluid exchange. For each model, we change the value of pseudo capillary pressure of vug system to match the results from corresponding fine-grid, single porosity simulation. Results are listed in Table 3.3. Noted that all these cases are mix wet models with the same matrix relative permeability curve and capillary pressure curve.

Table 3.3—Pseudo capillary pressure of vug system for various models

Vug Fraction		$\Delta P / \Delta L$	Height	No. of vugs	CSA	Pcap_vug
0.032		2.475	2.00	1	3.00	4.50
0.056		2.475	2.00	1	5.00	4.25
0.080		2.475	3.00	1	6.00	5.80
0.104		2.475	3.00	1	8.00	5.50
0.128		2.475	3.00	1	9.00	5.80
0.160		2.475	4.00	1	10.00	7.50
0.199		2.475	3.00	1	13.00	5.30
0.031		2.475	0.50	32	0.25	1.50
0.055		2.475	0.50	56	0.25	1.25
0.079		2.475	0.50	80	0.25	1.15
0.102		2.475	0.50	104	0.25	0.90
0.126		2.475	0.50	128	0.25	0.85
0.031		2.475	1.00	2	2.00	3.00
0.055		2.475	1.50	2	2.25	3.60
0.079		2.475	2.00	2	3.00	4.00
0.103		2.475	3.00	2	3.00	6.00
0.126		2.475	3.00	2	4.00	5.50
0.080		3.473	3.00	1	6.00	12.50
0.080		4.531	3.00	1	6.00	19.00
0.080		5.549	3.00	1	6.00	24.50
0.080		6.567	3.00	1	6.00	29.50
0.104		3.473	3.00	1	8.00	12.00
0.104		4.531	3.00	1	8.00	17.50
0.104		5.549	3.00	1	8.00	23.50
0.104		6.567	3.00	1	8.00	29.00
0.128		3.473	3.00	1	9.00	12.00
0.128		4.531	3.00	1	9.00	17.00
0.128		5.549	3.00	1	9.00	23.00
0.128		6.567	3.00	1	9.00	29.00

The multiple regression is applied on the history matching results, and indicates that the number of vugs per coarse cell and the cross section area of vug hardly have any impact on the value of psudo capillary pressure of vug system. As a result, the equation of pseudo capillary pressure of vug system in two-phase matrix-vug transfer function is expressed as:

$$P_{cap\_v} = A \bullet H_{vug} + B \bullet \frac{\Delta P}{\Delta L} + C \bullet F_v + D \tag{3.13}$$

Here, H_{vug} is the vug length along the direction of pressure gradient $\frac{\Delta P}{\Delta L}$, F_v is the vug fraction, A, B, C, D are constants that influenced by wettability, matrix capillary pressure, fluid density and so on. In this case, A = 2.00, B = 5.63, C = -7.22, D = -13.19.

To obtain the equation of pseudo capillary pressure for vug system, engineers should follow the process that described in Section 3.3.1 with basic petrophysical parameters of the interested reservoir at hand.

CPU computation time of the triple porosity simulation is shown to decrease significantly compared to that of fine-scale simulation.

3.4 A Novel Upscaling Method

As shown in **Fig. 3.28**, the triple porosity, coarse model tends to underestimate the oil recovery from fine-grid, single porosity model at later times. This is caused by numerical dispersion when upscaling 1000 fine grid blocks into one coarse grid block. Here we use a simple homogeneous model which only contains high permeability fracture grid blocks to illustrate the upscaling effect, which leads to the coarse model solution deviating from the solution of fine-grid model. The fine-grid model and upscaled coarse model are shown in **Fig. 3.29**. The water saturation in the top grid block, which is highlighted in **Fig. 3.29**, as a function of time are compared for these two models. Results shows a big difference between these two water saturation curves in **Fig. 3.30**.

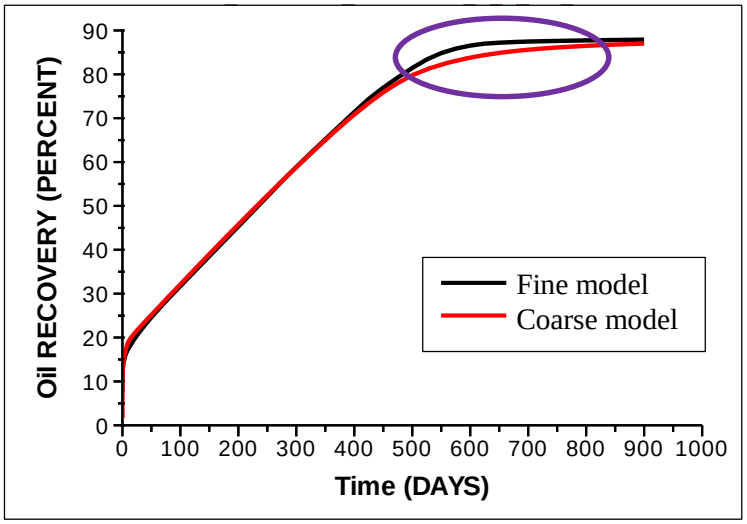

Fig. 3.28—Oil recovery vs. time for fine-grid, single porosity simulation and triple porosity simulation (purple circle shows the deviation)

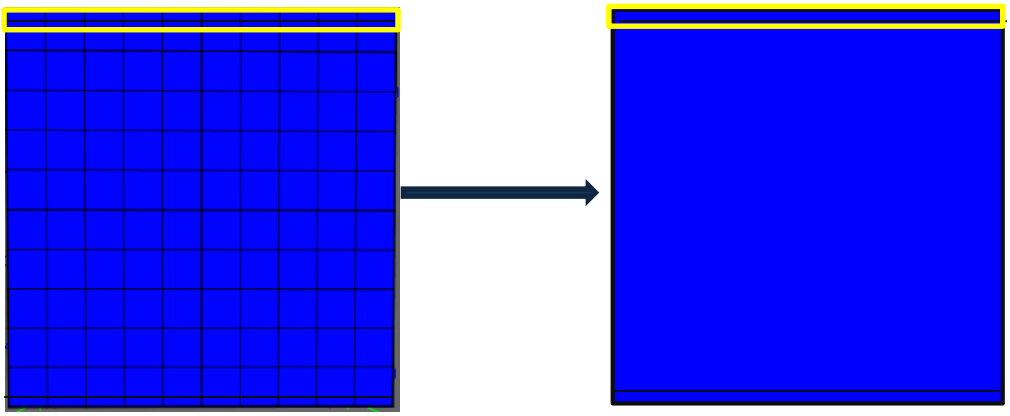

Fig. 3.29—Cross-section of homogeneous fine-grid model vs. coarse model

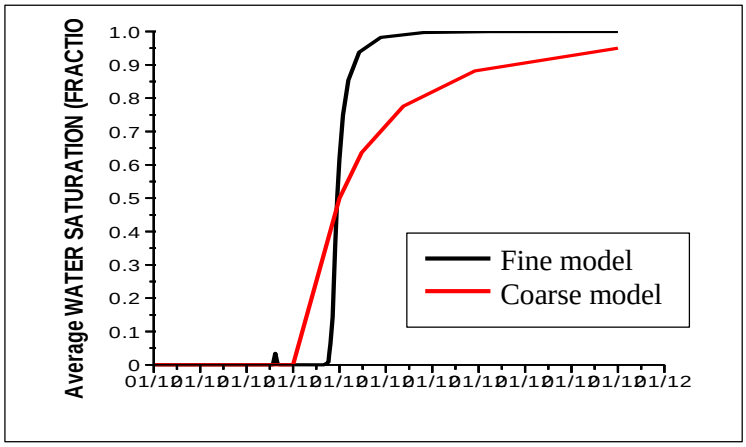

Fig. 3.30—Average water saturation in target grid block

To minimize the upscaling effect on coarse model, we proposed a transmissibility multiplier table for matrix system, which multiply the matrix transmissibility by specified constants as matrix water saturation increases. As we can see from **Fig. 3.28**, the difference between solutions from fine-grid model and coarse model exists in later times, so we only add multipliers to the matrix system beyond certain value of matrix water saturation, shown in Table 3.4.

Table 3.4—Transmissibility multiplier table

Sw-Swin	0	0.01	0.06	0.42	0.62
TAMULT	1	1	1	2.8	5

The matching result after applying proposed transmissibility multiplier table is shown in **Fig. 3.31**.

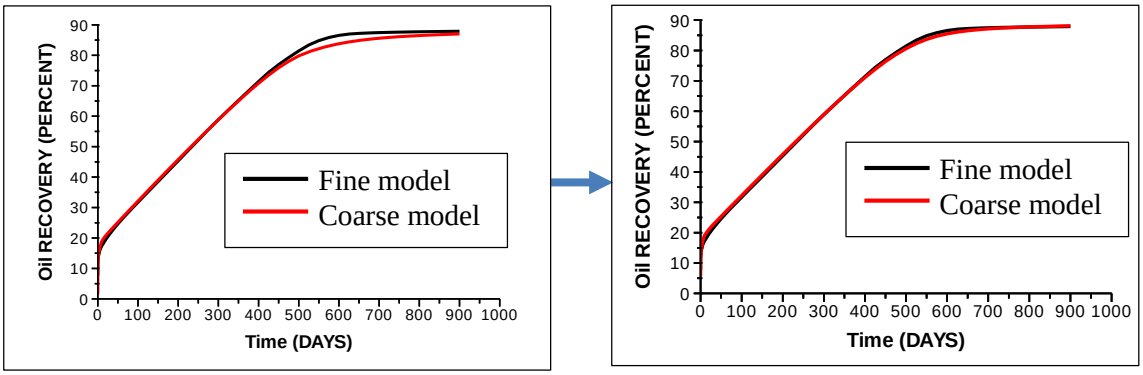

(a) Vug fraction = 10.4%

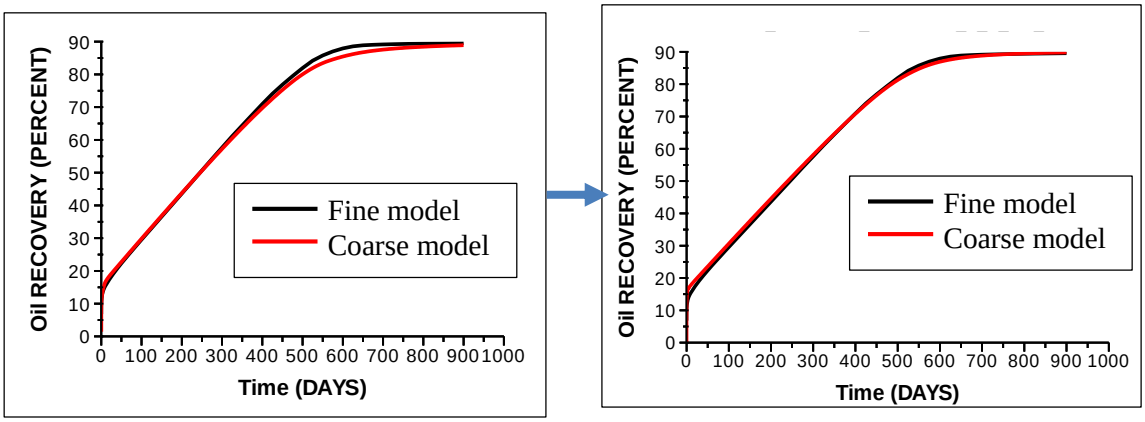

(b) Vug fraction = 12.8%

Fig. 3.31—Comparison of the matching results before (left) and after (right) applying transmissibility multiplier table

However, the disadvantage of adding this transmissibility multiplier table is the prohibitive computing cost. For example, the CPU computation time of the case with vug fraction of 12.8% increases from 60 seconds to 95 seconds after adding the transmissibility multiplier table. But it is still desirable comparing to the computation time of fine-grid model which takes more than 1 hour.

CHAPTER IV

FRACTURE-VUG TRANSFER FUNCTION

4.1 Model Introduction

In naturally fractured, vuggy reservoir, the presence of connected vugs can increase the reservoir permeability by orders of magnitude (Popov et al. 2007). Inability to model the fluid exchange between fractures and connected vugs will lead to a failure in the accurate prediction of the reservoir production. Since the fluid exchange between fractures and vugs drives the oil recovery in such reservoirs, the triple continuum model must incorporate an adequate fracture-vug transfer function.

Additional fractures are added to the previous conceptual models so that vug is connected to the global fracture network. As shown in **Fig. 4.1**, fractures can be located perpendicular or parallel to the fluid flow direction. And the number of fractures that are connected to the vug can be varied case by case. Since most of connected vugs are larger cavities with sizes of several centimeters in diameter (Yu-shu Wu et al., 2006), only representative models with single vug inside are considered in this chapter.

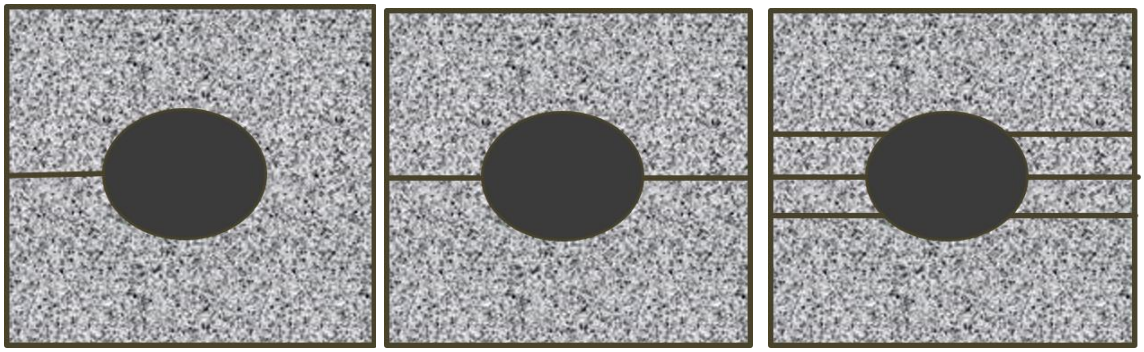

(a) Natural fractures perpendicular to the fluid flow direction

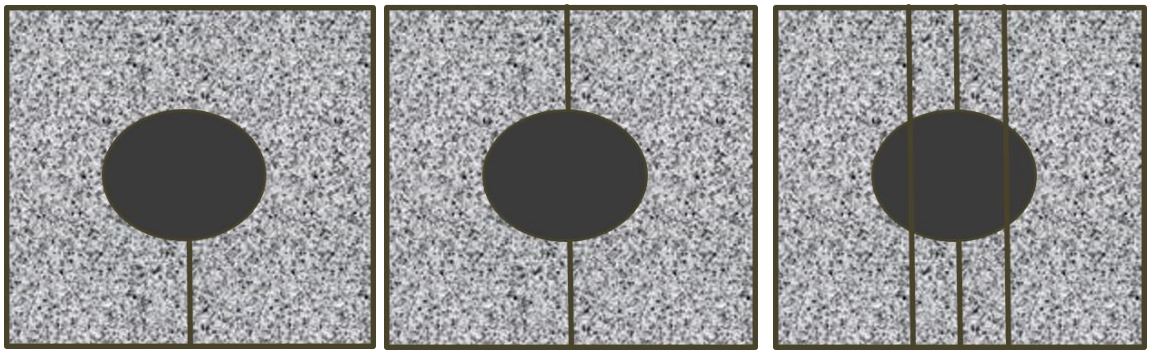

(b) Natural fractures parallel to the fluid flow direction

Fig. 4.1—Cross-section of conceptual models for fractured reservoirs with connected vugs

4.2 Mechanisms of Mass Transfer

As shown in **Fig. 4.2**, fractures that intersect the upper part of vug provide flow path for oil flowing out of vug, while fractures that intersect the lower part of vug offer channels for water flowing into vug. Pressure difference is the driving force of this fluid exchange. However, in triple continuum models, the pressure of fracture grid block is always lower than the pressure of vug grid block, prohibiting water flow into vug. A pseudo capillary pressure of vug system is needed in this case to provide a pseudo capillary force that allows water flow from fractures into vug. For this reason, we kept to

use the pseudo capillary pressure of vug system that obtained from matching the matrix-vug mass transfer in previous chapter, and by changing the shape factor in fracture-vug transfer function, a good match between oil recovery from the triple continuum model and the one from single porosity, fine-grid model is achieved.

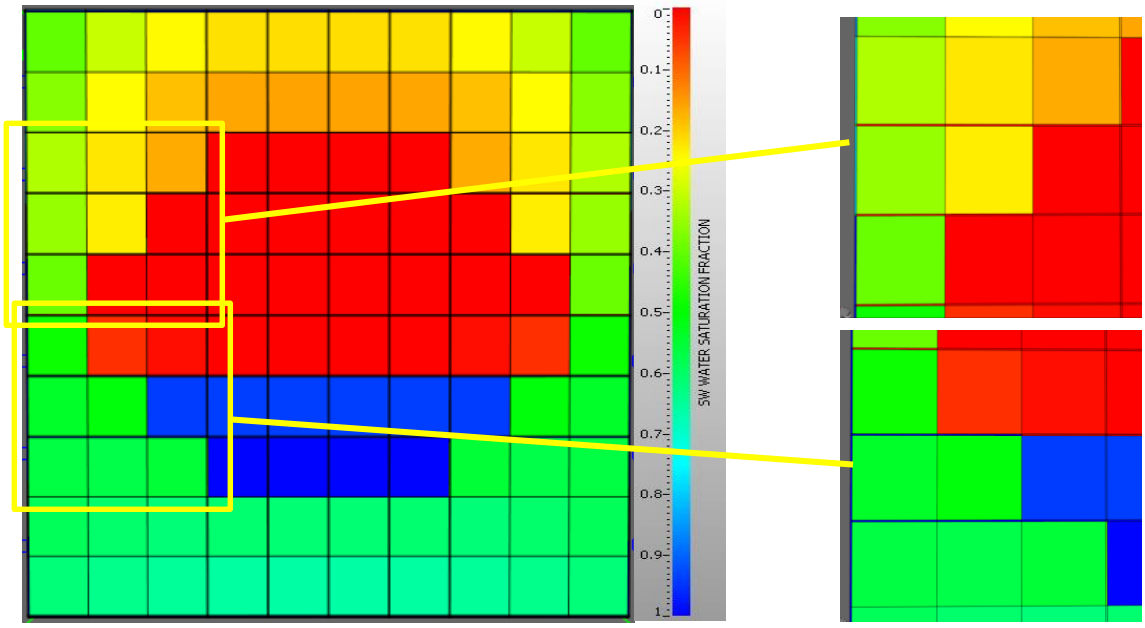

Fig. 4.2— Saturation profile of the fine-scale model at intermediate times

4.3 Effect of Vug Connectivity

Vug fraction is proven to have a great impact on fluid exchange between matrix and vug, however, whether it will influence the fluid exchange between fracture and vug is still unknown. Therefore, cases with vug fractions vary from 8.0%, 10.39% to 12.82% are created to investigate the effect of vug fraction on fracture-vug mass transfer. All three cases have one fracture connected to the vug at the same location shown in **Fig. 4.3**. In addition, they all have the same pseudo capillary pressure of vug system. Good

agreements between fine-grid simulation solutions and triple continuum simulation solutions are achieved for all three cases at the same shape factor of 0.000009. See **Fig. 4.3** for the matched oil recovery curves. It can be concluded that the value of shape factor in fracture-vug transfer function is not depend on vug fraction. This is reasonable based on the fact that the contact area between fracture and vug is so small that can be treated as a point, and that the pressure difference acting on the fluid exchange is the same when fractures are connected to the vug at the same height.

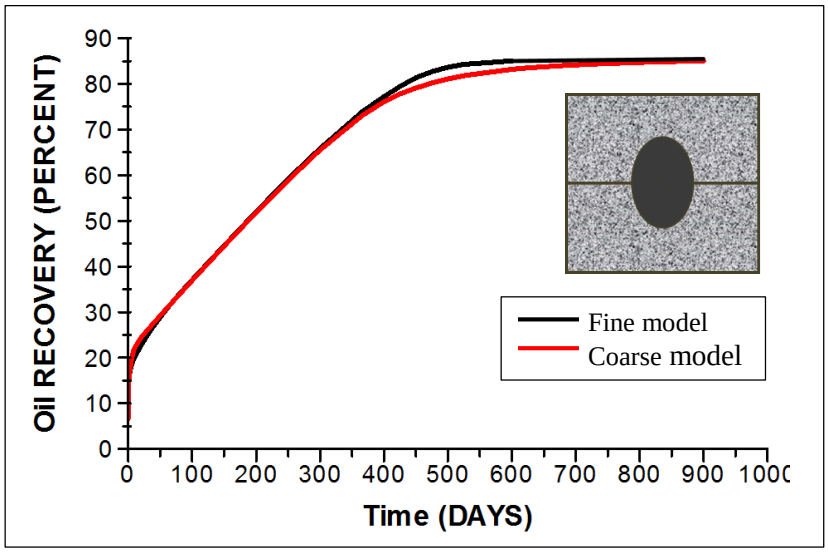

(a) Vug fraction = 8.0%

Fig. 4.3— Oil recovery vs. time for fine-grid, single porosity simulation and triple continuum simulation for various vug fraction cases

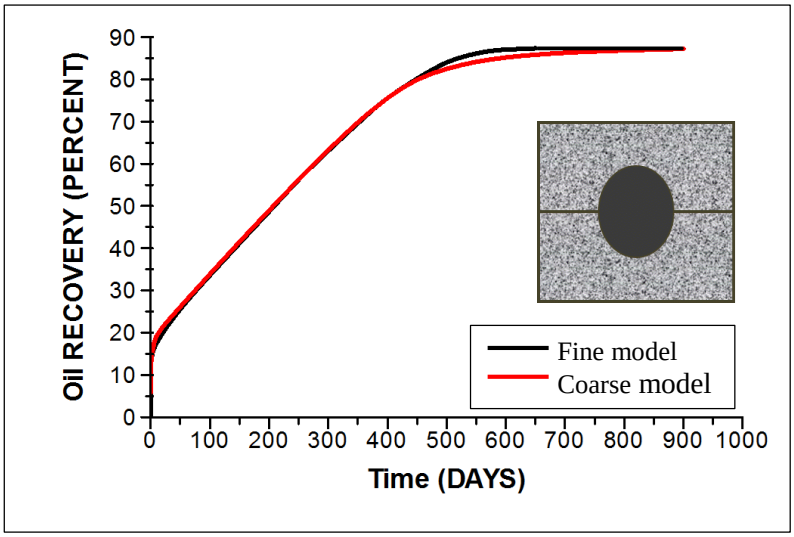

(b) Vug fraction = 10.4%

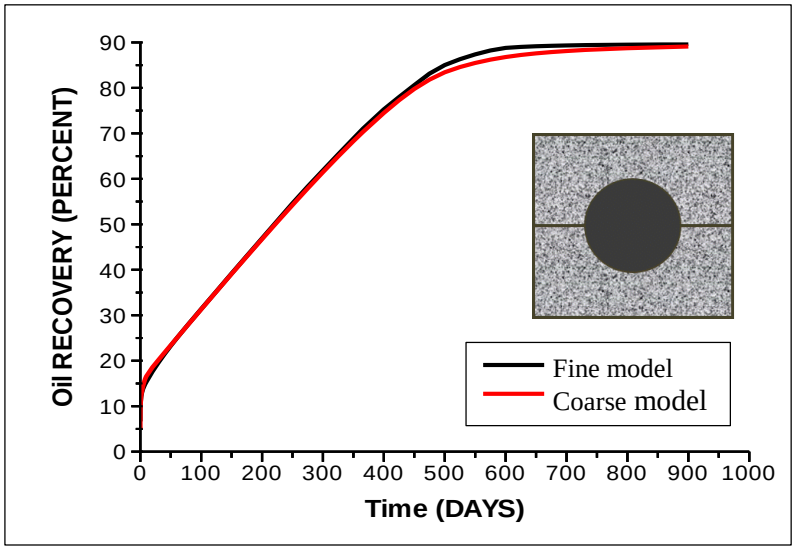

(c) Vug fraction = 12.8%

Fig. 4.3— Continued

Since pressure difference is the driving force for fracture-vug mass transfer, the way that fractures interact with a vug could influence the value of driving force and thus have a significant impact on oil displacement from vug system. To investigate its effect,

two representative models, one with a fracture connected the vug at the direction perpendicular to pressure gradient (fluid flow direction) and another at the direction parallel to pressure gradient, are established. The oil recovery curves corresponding to different fracture directions are plotted in **Fig. 4.4**. As can be seen, the representative model that has a fracture perpendicular to pressure gradient is shown to have much lower oil recovery rate than the one with a fracture parallel to pressure gradient. Sensitivity analysis are performed by varying the number of fractures that connected to the vug for both cases. The results show that the oil recovery increases as the number of fractures connected to the vug increases (**Fig. 4.5** and **Fig. 4.6**).

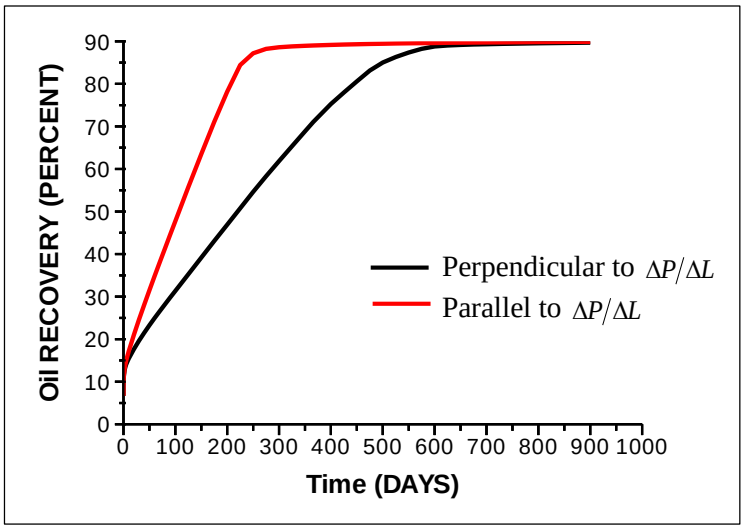

Fig. 4.4— Effect of the direction at which a fracture connected the vug

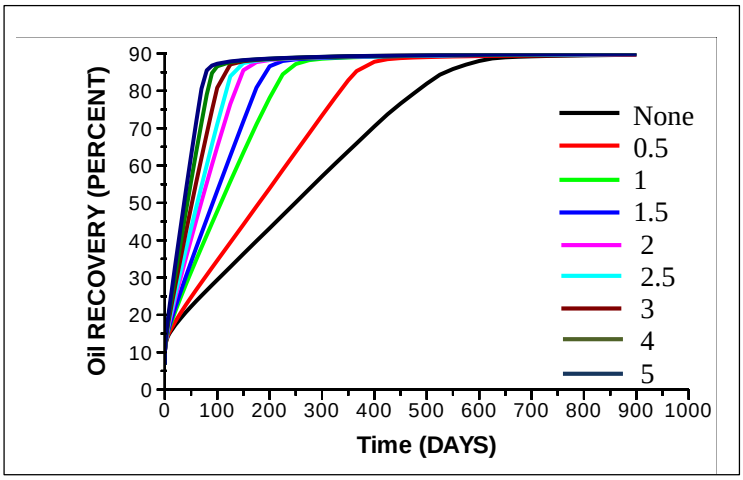

Fig. 4.5— Sensitivity to the number of fractures (connected to the vug) that are parallel to pressure gradient

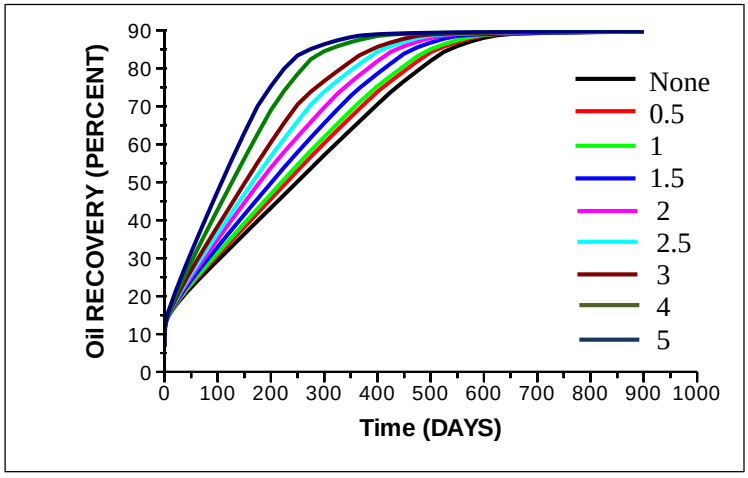

Fig. 4.6— Sensitivity to the number of fractures (connected to the vug) that are perpendicular to pressure gradient

4.4 Fracture-vug Transfer Function

The previous section has demonstrated the effect of fracture direction on oil recovery. Therefore, two scenarios, one with fractures perpendicular to the pressure gradient direction and another parallel to the pressure gradient direction, should be

discussed separately. For each scenario, models with various number of fractures intersecting the vug and different pressure gradient are designed to determine the equation of shape factor in fracture-vug transfer function. By changing the value of shape factor, a good agreement can be achieved between oil recoveries from triple continuum model and fine-scale model. The matching results of two example cases with different fracture directions are shown in **Fig. 4.7** and **Fig. 4.8**.

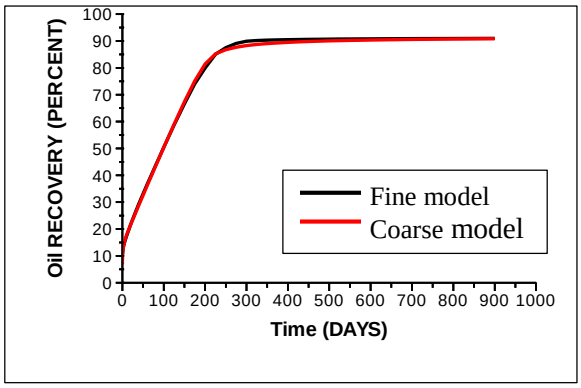

(a) Vug is connected by one fracture

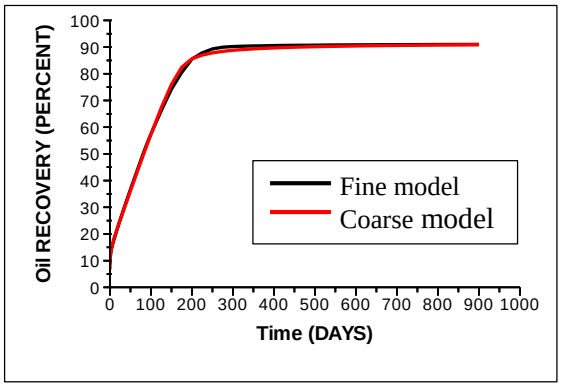

(b) Vug is connected by two fractures

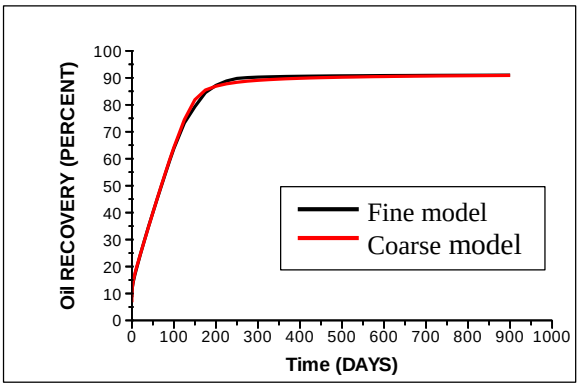

(c) Vug is connected by three fractures

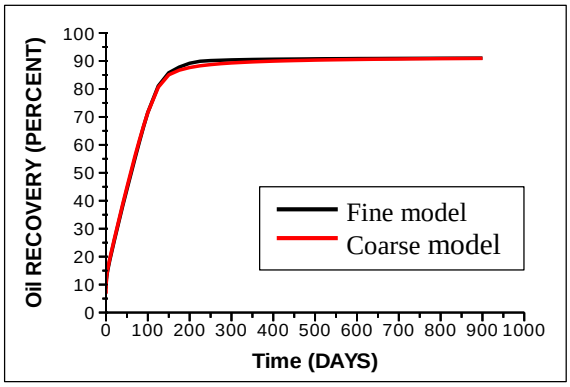

(d) Vug is connected by four fractures

Fig. 4.7— Oil recovery vs. time for models with fractures perpendicular to the pressure gradient (4.545 psi/ft)

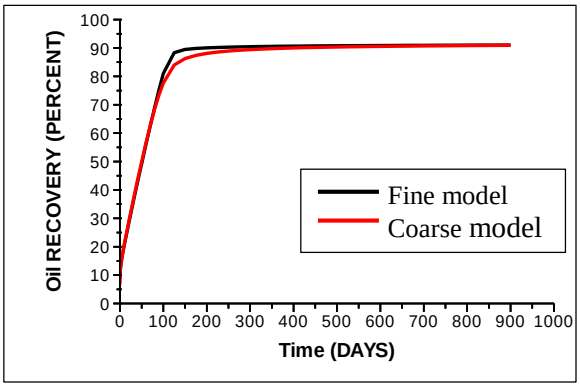

(a) Vug is connected by one fracture

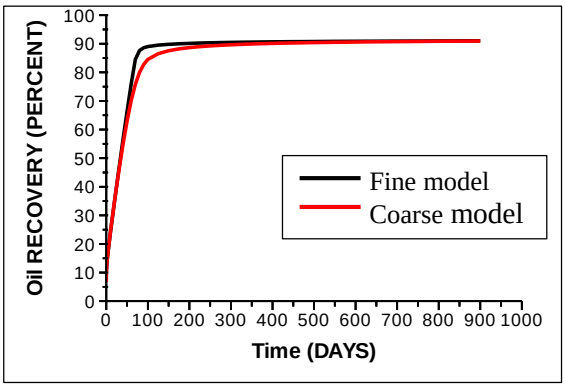

(b) Vug is connected by two fractures

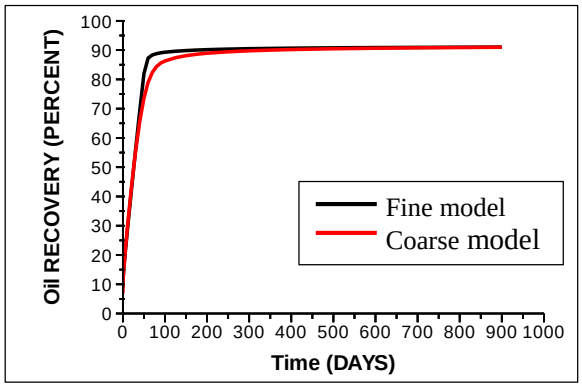

(c) Vug is connected by three fractures

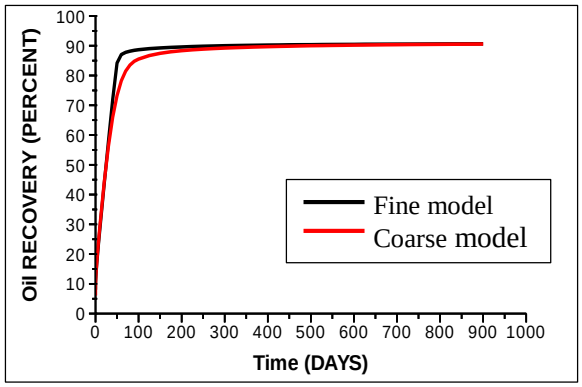

(d) Vug is connected by four fractures

Fig. 4.8— Oil recovery vs. time for models with fractures parallel to the pressure gradient (4.545 psi/ft)

Repeat the process mentioned above until all the models have been matched. Table 4.1 illustrated the history matching results for cases with fractures perpendicular to the pressure gradient. Here, the value of shape factor changes with the number of fractures, pressure gradient and pseudo capillary pressure of vug system.

Table 4.1—Shape factor for models with fractures perpendicular to the pressure gradient direction

No. of fractures	$\Delta P / \Delta L$	Pcap_vug	$\Delta P / \Delta L / P_{cap\_vug}$	Shape factor
0.5	2.470356	6.1	0.404976	0.000035
1	2.470356	6.1	0.404976	0.00014
1.5	2.470356	6.1	0.404976	0.00018
2	2.470356	6.1	0.404976	0.0003
2.5	2.470356	6.1	0.404976	0.0004
3	2.470356	6.1	0.404976	0.0005
4	2.470356	6.1	0.404976	0.00068
5	2.470356	6.1	0.404976	0.00085
0.5	3.525494	11.5	0.306565	0.00003
1	3.525494	11.5	0.306565	0.00011
1.5	3.525494	11.5	0.306565	0.00017
2	3.525494	11.5	0.306565	0.00024
2.5	3.525494	11.5	0.306565	0.00031
3	3.525494	11.5	0.306565	0.00038
4	3.525494	11.5	0.306565	0.00051
5	3.525494	11.5	0.306565	0.00063
0.5	4.545455	17	0.26738	0.00003
1	4.545455	17	0.26738	0.0001
1.5	4.545455	17	0.26738	0.000135
2	4.545455	17	0.26738	0.0002
2.5	4.545455	17	0.26738	0.00026
3	4.545455	17	0.26738	0.00033
4	4.545455	17	0.26738	0.00045
5	4.545455	17	0.26738	0.00056
0.5	5.556324	24	0.231514	0.000025
1	5.556324	24	0.231514	0.00009
1.5	5.556324	24	0.231514	0.00012
2	5.556324	24	0.231514	0.00018
2.5	5.556324	24	0.231514	0.00023
3	5.556324	24	0.231514	0.00028
4	5.556324	24	0.231514	0.00037
5	5.556324	24	0.231514	0.00047

Nonlinear regression is applied to get the equation of shape factor in fracture-vug transfer function:

$$\sigma = A \bullet \frac{\Delta P/\Delta L}{P_{cap\_vug}} \bullet N_f^B \tag{4.1}$$

Here, $\Delta P/\Delta L$ is the pressure gradient, P_{cap_vug} is the pseudo capillary pressure of vug system, N_f is the number of fractures connected to the vug, A and B are constants, in this case A=1.32, B=2.84*10^4.

The underlying reason for this form of shape factor equation may be due to the fact that the mass exchange between fracture and vug in coarse model is equivalent to the total mass exchange in fine-grid model.

$$\sum_1^{N_f} k_v \lambda_\alpha \left[\left(P_\alpha - \gamma_\alpha D \right)_f - \left(P_\alpha - \gamma_\alpha D \right)_v \right] = \sigma k_v \lambda_\alpha \left[\left(P_\alpha - \gamma_\alpha D \right)_f - \left(P_\alpha - \gamma_\alpha D \right)_v + P_{cap\_vug} \right] \tag{4.2}$$

For cases that have fractures parallel to the pressure gradient, Table 4.2 illustrated the history matching results with the shape factor value corresponding to different number of fractures, pressure gradient and pseudo capillary pressure of vug system.

Using nonlinear regression approach, the equation of shape factor in fracture-vug transfer function can be expressed as:

$$\sigma = A \bullet \frac{\Delta P/\Delta L}{P_{cap\_vug}} \bullet N_f^B + C \tag{4.3}$$

Here, A=2.13*10^{-5}, B=1.73, C=3.05*10^{-6}

Table 4.2—Shape factor for models with fractures parallel to the pressure gradient direction

No. of fractures	$\Delta P / \Delta L$	Pcap_vug	$\Delta P / \Delta L / P_{cap\_vug}$	Shape factor
0.5	2.470356	6.1	0.404976	0.000005
1	2.470356	6.1	0.404976	0.000009
1.5	2.470356	6.1	0.404976	0.00002
2	2.470356	6.1	0.404976	0.000033
2.5	2.470356	6.1	0.404976	0.000045
3	2.470356	6.1	0.404976	0.00006
4	2.470356	6.1	0.404976	0.000092
5	2.470356	6.1	0.404976	0.00013
0.5	3.525494	11.5	0.306565	0.000005
1	3.525494	11.5	0.306565	0.000009
1.5	3.525494	11.5	0.306565	0.000015
2	3.525494	11.5	0.306565	0.000025
2.5	3.525494	11.5	0.306565	0.000036
3	3.525494	11.5	0.306565	0.000046
4	3.525494	11.5	0.306565	0.000071
5	3.525494	11.5	0.306565	0.000102
0.5	4.545455	17	0.26738	0.000005
1	4.545455	17	0.26738	0.000009
1.5	4.545455	17	0.26738	0.000017
2	4.545455	17	0.26738	0.000026
2.5	4.545455	17	0.26738	0.000034
3	4.545455	17	0.26738	0.000043
4	4.545455	17	0.26738	0.000065
5	4.545455	17	0.26738	0.00009
0.5	5.556324	24	0.231514	0.000005
1	5.556324	24	0.231514	0.000008
1.5	5.556324	24	0.231514	0.000016
2	5.556324	24	0.231514	0.0000245
2.5	5.556324	24	0.231514	0.000032
3	5.556324	24	0.231514	0.000039
4	5.556324	24	0.231514	0.000059
5	5.556324	24	0.231514	0.000083

CHAPTER V

CONCLUSIONS

This work aims to solve the three challenges mentioned in Chapter 1, and provides a unified theory for the use of transfer functions in upscaling fractured, vuggy reservoir simulation models. The results developed in this work provide a new practical insight to the complex interporosity flow between three very different media in fractured, vuggy reservoirs.

(1) The results of sensitivity analyses show that the oil recovery from isolated vugs depends on vug fraction and vug number per coarse gird block. Using the fine-grid, single porosity model as a benchmark, and based on the history matching results, the equation of shape factor is established and found to be linearly correlated to $F_v \frac{1}{L_x^2}$. For case with different vug number, the coefficient of this linear correlation should be different. Those correlations developed on the basis of numerous simulation runs allow the estimation of shape factor for single-phase matrix-vug mass transfer.

(2) The dominant mechanisms of multiphase fluid exchange between matrix and vug are viscous forces, capillary forces and fluid expansion. Gravity forces may play an important role when the vug has a very large height. To incorporate all these mechanisms, a pseudo capillary pressure for vug system

as a function of pressure gradient, vug height and vug fraction is generated as a dynamic matrix-vug transfer function through a well-designed approach.

(3) A novel upscaling method is proposed to improve the accuracy of triple-continuum, coarse model by introducing a transmissibility multiplier table as another connection term for the transfer function.

(4) The two-phase fluid exchange between fracture system and vug system depends on the number of fractures connected to the vug as well as the fracture direction with respect to the pressure gradient, but has little to do with the vug fraction. For this reason, cases with fractures perpendicular to and parallel to the direction of pressure gradient should be considered separately. Following a well-designed procedure, the shape factor in fracture-vug transfer function as a function of pressure gradient and the number of fractures connected to the vug are obtained. Combined this shape factor with proposed pseudo capillary pressure of vug system gives the fracture-vug transfer function.

(5) The use of proposed transfer functions in triple-continuum models helps to reduce the size of simulation models, improve the computational efficiency by orders of magnitude for the simulation of FVRs on the field scale, while providing an accurate representation of the fine-scale results.

(6) Based on the methodology proposed in this research, an easy-to-use tool should be developed for reservoir engineers to generate transfer functions automatically.

REFERENCES

Abdassah, D. and I. Ershaghi 1986. Triple-Porosity Systems for Representing Naturally Fractured Reservoirs, published in SPEJ.

Abushaikha, A. S. and O. R. Gosselin 2008. Matrix-Fracture Transfer Function in Dual-Media Flow Simulation: Review, Comparison and Validation, Society of Petroleum Engineers, SPE-113890-MS presented at the SPE Europec/EAGE Conference and Exhibition, 9-12 June 2008, Rome, Italy.

Arbogast, T. and Lehr, H. L. 2006. Homogenization of a Darcy-Stokes System Modeling Vuggy Porous Media. Comput. Geosci., 10(3):291-302.

Barenblatt, G. I., I. P. Zheltov and I. N. Kochina 1960. "Basic concepts in the theory of seepage of homogeneous liquids in fissured rocks [strata]." Journal of Applied Mathematics and Mechanics (245): 1286-1303.

Camacho-Velazquez, R., M. Vasquez-Cruz, R. Castrejon-Aivar, abd V. Arana-Ortiz, Pressure transient and decline-curve behavior in naturally fractured vuggy carbonate reservoirs, SPE Reservoir Evaluation & Engineering, 95-111, April, 2005.

Carlson, E. S. and G. V. Latham 1993. Discrete Network Modeling For Tight Gas Fractured Reservoirs, SPE-26122-MS.

Chilingar, G. V., Mazzullo, S. J., Rieke, Herman H., Dominguez, G. C., Samaniego V., F., Cinco-L, Heber. 1996. Carbonate reservoir characterization : a geologic-engineering analysis. Part II, Amsterdam ; Oxford : Elsevier.

DeGraff, J. M., M. E. Meurer, L. H. Landis and S. L. Lyons 2005. Fracture Network Modeling and Dual-Permeability Simulation of Carbonate Reservoirs, International Petroleum Technology Conference, IPTC-10954-MS.

Dershowitz, W. S. and P. R. La Pointe 2007. Discrete Fracture Network Modeling For Carbonate Rock, American Rock Mechanics Association.

Gilman, J.R. and Kazemi, H., Aug 1983. Improvements in Simulation of Natually Fractured Reservoirs, published in SPEJ.

Gulbransen, A. F., V. L. Hauge and K.-A. Lie 2009. A Multiscale Mixed Finite Element Method For Vuggy and Naturally Fractured Reservoirs, SPE-119104-MS presented at SPE Reservoir Simulation Symposium, 2-4 February, The Woodlands, Texas.

Jennings, J. W., Jr. and F. J. Lucia 2001. Predicting Permeability From Well Logs in Carbonates With a Link to Geology for Interwell Permeability Mapping, SPE-71336-MS, presented at SPE Annual Technical Conference and Exhibition, 30 September-3 October, New Orleans, Louisiana.

Jie He, John E. Killough, Mohamed M. Fadlelmula F., Michael Fraim, 2015. Unified Finite Difference Modeling of Transient Flow in Naturally Fractured Carbonate Karst Reservoirs—A 3D Case Study. SPE-175098-MS, paper presented during the SPE Annual Technical Conference and Exhibition, 28-30 September, Houston, TX, USA

Jie He, John E. Killough, Mohamed M. Fadlelmula F., Michael Fraim, 2015. A Unified Finite Difference Model for the Simulation of Transient Flow in Naturally Fractured Carbonate Karst Reservoirs. SPE-173262-MS, paper presented during the SPE Reservoir Simulation Symposium, 23-25 February, Houston, TX, USA

Kang, Z., Y.-S. Wu, J. Li, Y. Wu, J. Zhang and G. Wang 2006. Modeling Multiphase Flow in Naturally Fractured Vuggy Petroleum Reservoirs, SPE-102356-MS, presented at SPE Annual Technical Conference and Exhibition, 24-27 September, San Antonio, Texas, USA.

Kazemi, H., L. S. Merrill, Jr., K. L. Porterfield and P. R. Zeman 1976. Numerical Simulation of Water-Oil Flow in Naturally Fractured Reservoirs, published in SPEJ, SPE-5719-PA.

Kossack, C. A. 2006. Simulation of Gas/Oil Displacements in Vuggy and Fractured Reservoirs, SPE-101674-MS, presented at SPE Annual Technical Conference and Exhibition, 24-27 September, San Antonio, Texas, USA.

Kossack, C. A. and O. Gurpinar 2001. A Methodology for Simulation of Vuggy and Fractured Reservoirs, SPE-66366-MS, presented at SPE Reservoir Simulation Symposium, 11-14 February, Houston, Texas.

Lim, K. T. and K. Aziz 1995. "Matrix-fracture transfer shape factors for dual-porosity simulators." Journal of Petroleum Science and Engineering 13(3–4): 169-178.

Liu, J., G. S. Bodvarsson and Y.-S. Wu 2003. "Analysis of flow behavior in fractured lithophysal reservoirs." Journal of Contaminant Hydrology 62–63(0): 189-211.

Lucia, F. J. 1999. Carbonate Reservoir Characterization, Springer-Verlag, Berlin.

Lucia, F. J. 2007. Carbonate reservoir characterization : an integrated approach, Berlin ; New York : Springer, [2007].

Parney, R., Cladouhos, T., La Pointe, P., Dershowitz, W., Curran, B. 2000. Fracture and Production Data Integration Using Discrete Fracture Network Models for Carbonate Reservoir Management, South Oregon Basin Field, Wyoming, SPE-60306-MS, presented at SPE Rocky Mountain Regional/Low-Permeability Reservoirs Symposium and Exhibition, 12-15 March, Denver, Colorado.

Popov, P., L. Bi, Y. Efendiev, R. E. Ewing, G. Qin, J. Li and Y. Ren 2007. Multi-physics and Multi-scale Methods for Modeling Fluid Flow Through Naturally-Fractured Vuggy Carbonate Reservoirs, SPE-105378-MS, presented at SPE Middle East Oil and Gas Show and Conference, 11-14 March, Manama.

Quandalle, P., Sabathier, J. C. 1989. Typical Features of a Multipurpose Reservoir Simulator, SPERE.

Ricardo Casar-González, and Vinicio Suro-Pérez 2000. Stochastic Imaging of Vuggy Formations, SPE-58998-MS, presented at the International Petroleum Conference and Exhibition in Mexico, 1-3 Feburary 2000.

Thomas, L.K., Dixon, T.N. and Pierson, R.G., Aug. 1983. Fractured Reservoir Simulation, published in SPEJ.

Warren, J. E. and P. J. Root 1963. The Behavior of Naturally Fractured Reservoirs, published in SPEJ, SPE-426-PA.

Wu, Y.-S., G. Qin, R. E. Ewing, Y. Efendiev, Z. Kang and Y. Ren 2006. A Multiple-Continuum Approach For Modeling Multiphase Flow in Naturally Fractured Vuggy Petroleum Reservoirs, SPE-104173-MS, presented at International Oil & Gas Conference and Exhibition in China, 5-7 December, Beijing, China.

Yan, B., Killough, J.E., Wang, Y. et al. 2013b. Novel Approaches for the Simulation of Unconventional Reservoirs. Society of Petroleum Engineers. DOI: 10.1190/URTEC2013-131.

Yan, B., Wang, Y., and Killough, J.E. 2015. Beyond Dual-Porosity Modeling for the Simulation of Complex Flow Mechanisms in Shale Reservoirs. Computational Geosciences: 1-23. DOI: 10.1007/s10596-015-9548-x